AN EXPERIMENTAL STUDY ON COBALT BASED CATALYTIC DRY REFORMING OF METHANE CATALYSTS

by

Cansu Yassı

B.S., Chemical Engineering, İstanbul Technical University, 2010

Submitted to the Institute for Graduate Studies in
Science and Engineering in partial fulfillment of
the requirements for the degree of
Master of Science

Graduate Program in Chemical Engineering

Boğaziçi University

2014

AN EXPERIMENTAL STUDY ON COBALT BASED CATALYTIC DRY REFORMING OF METHANE CATALYSTS

APPROVED BY:

Prof. Ahmet Erhan Aksoylu (Thesis Supervisor)	……....
Assoc. Prof. Hasan Bedir	.....…….....
Prof. Ramazan Yıldırım	……...

DATE OF APPROVAL: 17.01.2014

to my family

ACKNOWLEDGEMENTS

First and foremost, I would like to express my deepest gratitude to my thesis supervisor Prof. Ahmet Erhan Aksoylu for his support, guidance, patience, motivation and encouragement. Even for diffucult problems to be solved, he trusted in me. His guidance not only for my work but also for perspective in events was invaluable and it was a great honor for me to work with him during my thesis.

I wish to express my sincere gratitude to Dr. Burcu Selen Çağlayan who deserve special thanks for her excellent guidance, caring, willing to help and give her best suggestions throughout my work. Her guidance helped and motivated me in all the time of research and writing of this thesis.

I am very grateful to my thesis committee members; Prof. Ramazan Yıldırım and Assoc. Prof. Hasan Bedir for kindly revising and commenting on my thesis.

I would like to express my great appreciations for Assoc. Prof. Ahmet Kerim Avcı who devoted his valuable time to help me whenever I needed and Prof. Zeynep İlsen Önsan. It was a great opportunity for me to learn from their experiences.

Very special thanks goes to my friends Merve Eropak, Selcen Başar, Ali Uzun, Özge Ertem, Kerem Aksakal, İpek Paksoy and Aybüke Leba for their friendship and endless support throughout my master education without any hesitation.

I would also like to thank Serhat Erşahin, Burcu Karagöz, Sezin Sezen, Yeşim Düşova Teke, Elif Erdinç, Hazal Bal, Oya Gürsoy Yılmaz, Selen Solak and all my friends in Chemical Engineering Department at Boğaziçi University.

Cordial thanks are for Bilgi Dedeoğlu, and Yakup Bal for their technical assistance and help during my thesis.

Words cannot express how greatful I am to my beloved family; my father Selim Uğur Yassı, my mother Nezihe Yassı, my brother Onur Yunus Yassı, my aunt Hacer Çakmak and my cousin Çilem Çakmak. They always loved, encouraged, supported and believed in me unconditionally. They were always patience whenever I was dispirited. They always did their best for me. This thesis would not have been possible without their everlasting support. I dedicated this work to them.

I would also like to thank all other members of our family, especially my grandmother, Melahat Yassı for her prayers and my grandfather Enver Yassı. Even he passed away years ago, he keeps inspiring me with his personality and academic success.

I should add Benek, my cat, to the thank list. She never left me alone while I was studying even she felt sleepy.

Last, but by no means least, I would like to thank my boyfriend Ömür Akdağ. He was always there cheering me up and stood by me through the good times and bad. He was my support in the moments when there was no one to answer my queries.

Financial support provided by TÜBİTAK through project 111M144 and Boğaziçi University through the project BAP M6755 are greatly acknowledged.

ABSTRACT

AN EXPERIMENTAL STUDY ON DESIGN, DEVELOPMENT AND TESTING OF CATALYTIC DRY REFORMING OF METHANE CATALYSTS

The aim of this study is to design Co-based CDRM (catalytic dry reforming of methane) catalysts and to understand the CDRM reaction kinetics over their surface. The thesis consists of two parts. In the first part, a 5 wt% Co-2 wt% Ce/δ-Al_2O_3 catalyst was designed and tested for its CDRM performance. Temperature, CH_4/CO_2 feed ratio and space velocity were used as experimental parameters. In the second part, 10 wt% Co-2 wt% Ce/ZrO_2 catalyst was prepared and kinetic tests were conducted over the catalyst in order to obtain a power law type and plausible mechanistic rate expressions for CDRM. For both catalysts, Ce was used as a promoter in order to increase the oxygen storage capacity via controlling the electronic structure of the metals over the support. For Co-Ce/δ-Al_2O_3 the results have shown that the catalyst suffers from severe coke deposition and consequent activity loss. In the tests, increasing temperature increased the activity although at low temperatures catalyst deactivated relatively slower. CDRM did not occur on the catalyst for high space velocities (for W/F value of mL/h g-cat.) though for the space velocities of 10000 mL/h g-cat. and 20000 mL/h g-cat., almost the same initial performances were observed. The kinetic study over Co-Ce/ZrO_2 catalyst revealed that the reaction could be expressed by a simple power-law rate equation, with reaction order of 1.0751 for CH_4 and -0.0988 for CO_2, indicating that the reaction rate is proportional to the partial pressure of methane while there is a very small inhibition effect of carbon dioxide. This inhibition effect may be due to CO_2 and CH_4 competing for the same active sites. An ER mechanism having the reaction of adsorbed CO_2 with gas phase CH_4 leading directly to products, and an LH mechanism having surface reaction of the adsorbed reactants to form products H_2 and CO as the rate determining steps are found plausible. On the other hand, the results clearly indicate that further FTIR-DRIFT analysis is necessary for finding the mechanism of CDRM reaction on Co-Ce/ZrO_2 system. In the mixed feed tests to determine effect of product, the correlation coefficient (R^2) was found so small that any observation could not be possible.

ÖZET

METANIN KURU REFORMLANMASINDA KULLANILACAK KOBALT BAZLI KATALİZÖRLER HAKKINDA DENEYSEL ÇALIŞMA

Bu çalışmanın amacı metanın kuru reformlanmasında kullanılacak kobalt bazlı katalizörler tasarlamak ve katalizör yüzeyinde gerçekleşen reaksiyonun kinetiğini anlamaktır. Çalışma iki kısımdan oluşmaktadır. İlk kısımda ağırlıkça 5% Co-2% Ce/δ-Al_2O_3 katalizörü tasarlanmış olup katalizörün farklı sıcaklık, CH_4/CO_2 besleme oranları ve alan hızlarında performans analizi yapılmıştır. İkinci kısımda ağırlıkça 10% Co-2% Ce/ZrO_2 katalizörü hazırlanmış, metanın kuru reformlanması reaksiyonu için üssel hız denklemi ve mekanistik hız denklemleri elde etmek amacıyla kinetik testler gerçekleştirilmiştir. İki çalışmada da yardımcı metal olarak Ce kullanılmıştır. Ce, metallerin elektronik yapılarını kontrol ederek katalizörlerin oksijen depolama kapasitelerini arttırmaktadır. Co-Ce/δ-Al_2O_3 katalizörüyle ilgili çalışmalarda katalizörde karbon çökmesi nedeniyle aktivite kaybı görülmüştür. Sıcaklık artışının aktiviteyi arttırırken düşük sıcaklıklarda katalizör daha stabil bir performans göstermiştir. 30000 mL/saat g-katalizör alan hızında reaksiyon gözlenmezken 10000 mL/saat g-katalizör ve 20000 mL/saat g-katalizör alan hızları için benzer performanslar elde edilmiştir. Co-Ce/ZrO_2 katalizörü için gerçekleştirilen kinetik çalışmada reaksiyonun basit üssel hız denklemiyle ifade edilebildiği görülmüş ve metana ait reaksiyon katsayısı 1.0751, karbondioksite ait reaksiyon katsayısı -0.0988 bulunmuştur. Bu değerler reaksiyon hızının metanın kısmi basıncıyla doğru orantılı olduğunu, karbondioksitinse reaksiyonu az da olsa engellediğini göstermektedir. Bunun nedeni metan ve karbondioksitin katalizör yüzeyinde aynı aktif kısımlar için mücadelesi olabilir. Deneyler sonucunda, karbondioksition adsorblanıp metanın gaz fazda olduğu ER mekanizması ve reaktanların ikisinin de adsorblanarak ürünlere dönüştüğü LH mekanizması makul bulunmuştur. Reaksiyon kinetiğini detaylı olarak belirleyebilmek için FTIR-DRIFT analizlerine ihtiyaç vardır. Yapılan karma testler için oluşturulan denklemlerin korelasyon katsayısı düşük olduğudan herhangi bir yorum yapılamamıştır.

TABLE OF CONTENTS

LIST OF FIGURES

LIST OF TABLES

LIST OF SYMBOLS

Al_2O_3	Aluminum oxide
C_6H_{14}	Hexane
Ce	Cerium
CH_3OH	Methanol
CH_4	Methane
Co	Cobalt
CO	Carbon monoxide
CO_2	Carbon dioxide
E_{app}	Apparent activation energy
F	Total flow
$F(CH_4)$	Total flow of methane
Fe	Iron
g-cat	Catalyst weight in grams
h	Hour
H_2	Hydrogen
Ir	Iridium
K	Potassium
k_0	Preexponential factor
K_i	Adsorbtion constant
K_p	Equilibrium constant
La_2O_3	Lanthanum oxide
Li	Lithium
MgO	Magnesium oxide
min	Minute
mL	Milliliter
Mn	Manganese
Mo	Molydenum
n	Reaction order
$N(CH_4)$	CH_4 flow rate, mol/h
Ni	Nickel

Pd	Palladium
Pt	Platinum
R	Gas constant
$-r(CH_4)$	Reaction rate of methane
R^2	Correlation coefficient
Rh	Rhodium
Ru	Ruthenium
SiO_2	Silicon dioxide
T	Temperature
W	Catalyst weight
W/F	Space velocity
wt%	Weight percentage
$X(CH_4)$	Conversion of methane
ZrO_2	Zirconium oxide
α	Reaction rate order of methane
β	Reaction rate order of carbon dioxide
δ	Reaction rate order of carb n monoxide
γ	Reaction rate order of hydrogen
σ^2	Variance of the experimental error

LIST OF ACRONYMS/ABBREVIATIONS

CDRM	Catalytic Dry Reforming of Methane
CR	Combined Reforming
EDS (EDX)	Energy-dispersive X-ray Spectroscopy
ER	Eley Rideal
F-T	Fischer Tropsch
FTIR	Fourier Transform Infrared Spectroscopy
FTIR-DRIFT	Gas Hourly Space Velocity
GC	Gas Chromatography
LH	Langmiur Hinshelwood
LT-WGS	Low Temperature Water Gas Shift
MBSL	Multi-bubble Sonoluminescence
RDS	Rate Determining Step
SEM	Scanning Electron Microscope
TCD	Thermal Conductivity Detector
TEM	Transmission Electron Microscopy
TGA-DTA	Thermogravimetric/Differential Thermal Analyses
TPH	Temperature Programmed Hydrogenation
TPR	Temperature Programmed Reduction
TPSR	Temperature Programmed Surface Reaction
WGS	Water Gas Shift
XPS	X-ray Photoelectron Microscopy
XRD	X-ray Diffraction

1. INTRODUCTION

Global warming and rapidly depleting natural reserves due to abundant use of non-renewable fossil fuels like petroleum and coal have been a strong motivation for the studies on alternative power sources and greenhouse gases emmission minimization (Domínguez *et al.*, 2007, Fan *et al.*, 2011).

The natural gas, which has methane as the major component with a fraction of 70 to 98% depending on the location, is considered as the fuel of the near future due to its worldwide reserves. However, most of the natural gas reserves are situated in areas remote from the centers resulting in high costs of compression, transportation and storage. To make methane reserves economically more feasible, a large amount of research on the conversion of methane to liquids or hydrocarbons has been carried out. There have been studies on direct oxidative conversions of methane into methanol, formaldehyde, propanal, benzene and other aromatics, and direct oxidative coupling of methane to ethane and ethylene. However, the above processes suffer from low yield and are not economically feasible (Ozkara-Aydınoglu, 2008; Claridge *et al.*, 1998).

Current industrial processes make use of methane as a feedstock in production of synthesis gas, which is a mixture of CO and H_2. Synthesis gas, which is also called syngas, is further used for production of oxygenated compounds, methanol synthesis, for production of liquid hydrocarbons through Fischer-Tropsch (F-T) synthesis or several other carbonylation, hydrogenation and reduction processes (Ozkara-Aydınoglu, 2010).

Reforming of methane to syngas can be carried out in three different ways: steam reforming, partial oxidation and carbon dioxide reforming. Recently, carbon dioxide reforming of methane (catalytic dry reforming of methane) (CDRM) has gained attention. With this reaction, two greenhouse gases are converted into valuable syngas (Kanamori *et al.*, 2006). The products CO and H_2 with equal molar ratio are more suitable for the F-T synthesis compared to products of the steam reforming and partial oxidation of methane. In addition, dry reforming is also used for storing and transporting solar and atomic energy.

Consequently, the study on the design and development of CDRM is important in terms of environmental and industrial viewpoints (Cui *et al.*, 2007).

CDRM has been widely studied on supported group VIII metal catalysts. Noble metals such as Ru, Rh, Pd, Pt, Ir and non-noble metals like Ni, Co, Fe are found to be catalytically active. Noble metals are more active catalysts yielding low carbon deposition but they have limited availability and high cost. Although non-noble metals are less expensive and widely available, they are more rapidly deactivated via carbon deposition and/or metal sintering, which are the major drawbacks of CDRM as the reaction is strongly endothermic and it requires high temperatures, typically 800–900°C (Liu *et al.*, 2010).

These problems make researchers focus on developing catalysts with improved activity and selectivity which prevent or reduce the formation of surface carbon, guaranteeing long-term stable operation. This can be achieved by using different types of supports, preparation methods, or by addition of activity modifiers, such as noble or alkaline metals (Barroso-Quiroga *et al.*, 2010).

The overall purpose of this thesis is to design and develop an effective Co-based dry reforming catalyst to produce syngas under optimized reaction conditions. The thesis consists of two parts. In the first part, a 5 wt% Co-2 wt% Ce/δ-Al_2O_3 catalyst was designed and tested for its CDRM performance where temperature, CH_4/CO_2 feed ratio and space velocity are considered as the experimental parameters. In the second part, 10 wt% Co-2 wt% Ce/ZrO_2 catalyst was prepared and kinetic tests were performed in order to find the parameters of power-law type CDRM rate expression and to define plausible CDM mechanisms for the catalyst.

Chapter 2 involves a detailed literature survey on theorical background of carbon dioxide reforming of methane, catalyst deactivation mechanisms and kinetics of the reaction. Chapter 3 contains the experimental work carried out. The results obtained in the experiments are discussed in Chapter 4 and the conclusions drawn from the present study and recommendations for the future work are presented in Chapter 5.

2. LITERATURE SURVEY

Offering certain advantages over other reforming technologies like steam reforming (2.1) and partial oxidation (2.2), carbon dioxide reforming of methane (2.3) has received a lot of attention during the last few decades. The facts that not only CH_4 but also CO_2, both of which are greenhouse gases, are consumed in the CDRM and its H_2/CO product ratio being close to 1 are the major advantages of the reaction. Moreover, its products can be used in oxygenated compound production as well as the Fischer– Tropsch synthesis (Fidalgo *et al*., 2010; Ozkara-Aydınoglu *et al.*, 2009).

$$CH_4 + H_2O \leftrightarrow CO + 3H_2 \quad H_2/CO = 3 \quad \Delta H^0 = +206\ kj/mol \tag{2.1}$$

$$CH_4 + 1/2O_2 \leftrightarrow CO + 2H_2 \quad H_2/CO = 2 \quad \Delta H^0 = -38\ kj/mol \tag{2.2}$$

$$CH_4 + CO_2 \leftrightarrow 2CO + 2H_2 \quad H_2/CO = 1 \quad \Delta H^0 = +247\ kj/mol \tag{2.3}$$

Owing to its high endothermicity, CDRM can also be utilized in chemical energy transmission systems through the use of forward and reverse reaction as the parts of the endothermic-exothermic cycle. A power source generated from solar or nuclear energy can drive the reforming reaction and convert inexpensive energies into valuable chemical energy (Xu *et al.*, 2011).

Equations 2.4 and 2.5 give two examples of how the synthesis gas (syngas) obtained in dry reforming reaction can be used to produce sulfur-free diesel (C_6H_{14}) via Fischer-Tropsch synthesis and methanol (CH_3OH), respectively.

$$6CO + 13H_2 \rightarrow C_6H_{14} + 6H_2O \tag{2.4}$$

$$CO + 2H_2 \rightarrow CH_3OH \tag{2.5}$$

Both of these reactions require H_2 to be added to the reactant feed in order to adjust the H_2/CO ratio. The hydrogen required can be supplied from the steam reforming of

methane (Er-rbib *et al.,* 2012). This brings about the possibility of combining steam reforming, partial oxidation and dry reforming reactions to get the desired H_2/CO ratio for different applications (Rezaei *et al.,* 2007).

The low cost of CDRM is one of its most significant advantages. In fact, syngas can be produced not only from natural gas but also from a variety of primary feedstock such as coal, petroleum coke and biomass. The lowest cost routes for syngas production are based on natural gas. Since natural gas reservoirs contain primarily CH_4 but may have a large fraction of CO_2, CDRM which utilizes both CH_4 and CO_2 is a promising technology for syngas production from CH_4. However, there has not been a commercial CDRM-alone application yet (Stagg-Williams *et al*., 2000; Gangadharan *et al*., 2012).

The major challenge that hinders the development of dry reforming process commercially is the lack of an effective catalyst, which is able to operate efficiently under severe reaction conditions (Liu *et al.,* 2009). Due to the highly endothermic nature of the process, CDRM requires high temperatures which result in the rapid deactivation of the catalysts originating from the sintering of the metal active sites and the carbon deposition (Xu *et al.*, 2011).

The coke originates mainly from two reactions, carbon monoxide disproportionation (2.6) and methane decomposition (2.7). The former is an exothermic reaction is favored at lower temperatures and higher pressures whereas the latter is an endothermic reaction which is favored at higher temperatures and lower pressures (Al-Fatesh *et al.*, 2011). The thermodynamic analysis of these reactions shows that carbon deposition is favored in 500-800°C temperature range (Juan-Juan *et al*., 2009).

$$CO \leftrightarrow C + CO_2 \qquad \Delta H^0 = -172\ kj/mol \tag{2.6}$$

$$CH_4 \leftrightarrow C + 2H_2 \qquad \Delta H^0 = +75\ kj/mol \tag{2.7}$$

From the industrial standpoint, it is desired to develop catalysts with improved activity and selectivity in order to prevent or reduce the formation of carbon and/or sintering of the metallic phase and support to achieve long term stable operation. This can

be done by using different types of supports and preparation methods or by the addition of activity modifiers, such as noble or alkaline metals (Barroso *et al.*, 2010; Ozkara-Aydınoglu *et al.*, 2009).

2.1. Catalysts for CO_2 Reforming of CH_4

Catalytic systems employed in CDRM reaction can be categorized into two groups: Transition metal and noble metal-based catalysts (Souza *et al.*, 2001; Ruckenstein *et al.*, 2002; Rezaei *et al.*, 2006; Fan *et al.*, 2011; Ozkara-Aydınoglu *et al.*, 2009; Luisetto *et al.*, 2012). Compared to the former, the noble metal based catalysts were reported to exhibit excellent catalytic performances.

2.1.1. Noble Metal Based Catalysts

Many studies related to the reforming reaction of methane with CO_2 were conducted over noble metals in order to develop a successful catalyst and to gain an enhanced understanding of the mechanisms of reaction and deactivation. The result of these studies showed that the activity of noble metal catalysts can be attributed to the reduced mobility and/or solubility of carbon in noble metals (Bartholomew, 2001; Damyanova *et al.*, 2009; Ozkara-Aydınoglu *et al.*, 2009; Chen *et al.*, 2010).

Several factors such as the nature of the metal, the support type as well as the conditions for the catalyst preparation and pretreatment affect the catalytic performance of supported noble metal catalysts for CDRM reaction. In literature, it is indicated that support has a significant effect on both catalytic activity and stability. It has been shown that certain supports are able to provide oxygen to the metal during the reaction and, by this way, suppress carbon deposition. Thus, oxides with high oxygen exchange capacity and mobility are expected to be good candidates as supports for the CDRM reaction (Ozkara-Aydınoglu *et al.*, 2009).

In their study, Reddy *et al.* prepared $Pt/ZrO_2/SiO_2$ catalysts with different ratios of ZrO_2/SiO_2 mixed oxide supports (2:1 to 4:1) by using deposition–precipitation method. The synthesized catalysts along with Pt/ZrO_2 reference material were tested for CDRM at

800°C and at high space velocity. Among all the prepared catalysts, $Pt/ZrO_2/SiO_2$ (4:1) sample showed the highest activity. On the basis of X-ray diffraction (XRD) patterns, BET and H_2 chemisorption measurements, X-ray photoelectron and FTIR spectra, the better catalytic properties of the $Pt/ZrO_2/SiO_2$ (4:1) sample were explained by higher Pt dispersion due to the absence of free silica and the higher amount of amorphous $ZrSiO_4$ presence (Reddy *et al*., 2010).

Damyanova *et al.* investigated dry reforming over $Pt/CeO_2–ZrO_2$ catalysts with high surface area and mesoporous nanocrystalline zirconia carrier at atmospheric pressure. The effect of CeO_2 content (1–12 wt%) on the surface and catalytic properties of the catalysts were studied. It was observed that the morphology of Pt particles were influenced by the pre-treatment temperature and CeO_2 concentration. Authors reported that the small amount of CeO_2 up to 6 wt% had a stabilization effect on the textural properties of modified ZrO_2. Moreover, CeO_2 addition to Pt/ZrO_2 catalyst prevented catalyst deactivation by accelerating gasification of coke deposition on Pt particles. This was reported to be related to the increase of the oxygen mobility on the surface of the support due to close contact between Pt and ceria. In addition, it was noted that in order to prevent sintering, calcination temperature should be below 800°C (Damyanova *et al.*, 2009).

In their work, Chen *et al.* studied CDRM over $Ce_{0.75}Zr_{0.25}O_2$ solid solution supported Ru catalysts. The effect of Ru content on the properties of the catalysts was investigated. It was found that as Ru content exceeds 1.5 wt%, the surface areas and pore volumes of the catalysts decreased notably. H_2-Temperature programmed reduction (TPR) and XRD results showed that the interaction between Ru and the support increased with the decrease of Ru content. H_2-Temperature programmed desorption results releaved that the reduced support solid solution could store hydrogen, which was related to the formed anionic vacancy. The good catalyst stability was attributed to the carbon deposition resistance of metallic Ru, the redox role and the hydrogen storage capacity of the reduced support (Chen *et al*., 2010).

Nagaia *et al.* studied dry reforming of methane on the Rh/Al_2O_3 and Rh/CeO_2 catalysts. The experiments were performed using a flow microreactor at 500- 700°C. The effects of the catalyst pretreatment, the CH_4/CO_2 ratio and the CeO_2 support on the

catalytic performance of the catalyst were investigated. Results showed that the catalyst which was oxidized/reduced at 500°C had a higher activity than the oxidized-only catalyst. Moreover, CO_2 addition promoted the CH_4 reforming to form hydrogen and decreased the carbon deposition. The Rh/CeO_2 catalyst was found less active than the Rh/Al_2O_3 catalyst for CDRM; on the other hand, the carbon deposition was lower on the Rh/ CeO_2 catalyst. In addition, for the Rh/Al_2O_3 catalyst, increasing the temperature increased the formation rates of H_2 and CO, and the catalyst did not deactivate for at least 500 min (Nagaia *et al.*, 2007).

Addition of oxygen to the dry reforming process was found to reduce the carbon deposition on the catalytic surface and to increase the methane conversion (Nematollahi *et al*., 2011). Thus, the combination of CO_2 reforming and partial oxidation of methane is regarded as a promising process in synthesis gas production. In their study, Nematollahi *et al*. studied combined dry reforming and partial oxidation of methane to produce synthesis gas over noble metal catalysts supported on alumina-stabilized magnesia. BET measurements of the catalysts showed that compared to Ir and Pt catalysts; Ru, Rh, and Pd catalysts had higher specific surface area. It was observed that the methane conversion in combined reforming (CR) was higher than those observed in dry reforming and partial oxidation, and the H_2/CO ratio was around 0.7, 2 and 1 over different catalysts for CDRM, partial oxidation and CR reactions, respectively. The results obtained showed a high degree of activity for the ruthenium and rhodium catalysts and the following order of activity was observed for the catalysts: Rh = Ru > Ir > Pt > Pd (Nematollahi *et al*., 2011).

2.1.2. Transition Metal Based Catalysts

Although, the noble metal based catalysts exhibit excellent catalytic performances, the cost and availability of the noble metals limit their application. Thus transition metal-based catalysts are much more preferred. However, they encounter major drawback of catalyst deactivation caused by coke deposition as mentioned before (Fan *et al.*, 2011). Current research is mainly addressed to reduce carbon formation by: (i) choosing supports such as CeO_2 and CeO_2-ZrO_2 solid solutions with high mobility of oxygen ions that can react with adsorbed carbon species; (ii) modifying the surface properties with additives, such as potassium or sodium, that impart basic character, even though they lower the

catalytic activity; (iii) using multi-metallic catalysts. For example, the addition of precious metals (Pt, Rh, Ru) with nickel was reported to enhance both catalytic activity and long-term stability (Luisetto *et al*., 2012).

In particular, nickel and cobalt based catalysts have been intensively studied because of their low cost and relatively high activity in the reforming process (Juan-Juan *et al.*, 2009; Arkatova, 2010; Barroso-Quiroga *et al*., 2010; Fidalgo *et al.*, 2010; Daza *et al*., 2011; Eltejaei *et al*., 2012).

In literature, ZrO_2 is indicated as a reducible oxide material that can help to increase the carbon removal rate and clean carbon deposition on the metal surface (Yao *et al*., 2013). Besides, SiO_2 support is also widely used for promoted Ni-based catalysts in dry reforming reaction due to its good thermostability, availability and relatively high specific surface area. Yao *et al.* aimed to find out the effect of Mn and Zr promoters on the stability of Ni/SiO_2 catalyst for methane CO_2 reforming. Results exhibited that the introduction of Mn or Zr promoter increased the catalytic activity of the Ni/SiO_2 catalyst. The introduction of Mn enhanced the dispersion of the Ni species. Moreover, the $Ni\text{-}Mn/ SiO_2$ catalyst was found to be more resistant to coking. In contrast, the introduction of Zr increased the reducibility of the Ni/SiO_2 catalyst and more carbon deposition occurred with the decrease of reaction temperature, leading to severe deactivation at lower reaction temperatures over $Ni\text{-}Zr/SiO_2$ catalyst (Yao *et al.*, 2013).

In recent years, the use of carbon materials as catalyst supports has received attention. Among all types of carbon materials, activated carbon is the most commonly used one because besides its low cost, it has high mechanical resistance, high surface area and good reductive properties. The possibility of modifying surface chemistry and pore size distribution of activated carbon is highly advantageous considering the fact that through those modifications one can change the metal-support interaction and the properties of the activated carbon supported catalyst (Fidalgo *et al.*, 2010).

In their work, Fidelgo *et al.* studied the influence of drying method, reduction temperature and surface chemistry of the activated carbon used as supports for Ni catalyst. The results showed that oxidation of the carbon support enhanced the interaction between

Ni particles and carbon surface, and therefore Ni dispersion. In addition, Ni particle size was reported to be affected by the reduction temperature. It was found that the use of microwave drying instead of conventional oven drying decreased the operating time greatly and enabled the formation of smaller Ni particle sizes, and weakened the effect of surface chemistry on the Ni particle size (Fidalgo *et al.*, 2010).

Newnham *et al*. investigated Ni-mesoporous alumina catalysts for CDRM by using a new template assisted method which led to the production of a highly ordered, thermally stable support structure containing active Ni particles within the micropore channels. The catalysts were found significantly better than the ones prepared by wet impregnation/precipitation in terms of stability. The catalyst with intermediate Ni loading was found to have the highest activity among the materials studied. The appreciable activity and long term stability of these catalysts were contributed by the rigid, stable, high surface area nature of the support structure, high dispersion of the majority of metal nanoparticles within the alumina mesopores, and the prevention of active particle sintering within the mesopores (Newnham *et al.*, 2012).

The preparation of most heterogeneous catalysts requires calcination and reduction steps to decompose the metal precursor and to obtain the catalystic active metal, respectively. The final properties of the catalyst are strongly influenced by these treatments. Juan-Juan *et al*. studied the effects of the calcination and reduction treatments on the catalytic properties of a Ni/Al_2O_3 catalyst used in CDRM. They found out that the amount of carbon deposited was highly influenced by the pretreatment carried out. The pretreatments affected the size and structure of nickel particles significantly, and in general terms, the higher the mean particle size was, the higher was the amount of deposited carbon. The catalyst reduced at 700°C without prior calcination was reported to have the lowest carbon deposition meaning that the calcination pretreatment could be avoided for that particular catalyst (Juan-Juan *et al.*, 2009).

M.M. Barroso-Quiroga and Castro-Luna studied Ni-based CDRM catalysts which were prepared by impregnation on various ceramic oxides such as Al_2O_3, CeO_2, La_2O_3 and ZrO_2. The effect of modifiers like lithium and potassium oxides on the activity of Ni/CeO_2 catalyst was also studied. CDRM was carried out in a fixed-bed quartz reactor. Seven

catalysts were prepared by wet impregnation having 10 wt% Ni loading. The results exhibited that Ni/ZrO_2 showed a notable performance in CDRM reaction without catalyst deactivation. The highest methane conversion was observed for the Ni/CeO_2 catalyst. The unmodified catalyst was reported to have higher conversion values, although 0.5 wt% K and Li addition led to higher coke resistance ability (Barroso-Quiroga *et al.*, 2010).

In order to have better control of the coupled chemical reactions and resultant heat flow, cerium oxide (ceria), which is less active than Ni but has high resistance to carbon deposition compared to that of Ni, is a promising candidate as a promoter. Cerium oxide contains a high concentration of highly mobile oxygen vacancies and/or sinks for oxygen involved in surface reactions, and has a high resistance toward carbon formation. In literature, it was reported that under CDRM conditions, high surface area ceria, synthesized by a surfactant-assisted approach has provided significantly higher reforming reactivity and excellent resistance toward carbon deposition compared to Ni/Al_2O_3 and conventional low surface area ceria (Laosiripojana *et al.*, 2005).

The oxygen storage/transport capacity of ceria is known to decline under high temperatures and reductive conditions. Studies in literature showed that zirconia addition stabilizes ceria by forming a ceria–zirconia solid solution and improving textural features, thermal resistance, catalytic activity at lower temperatures and, the most importantly, oxygen storage/transport properties (Kambolis *et al.*, 2010). Ceria–zirconia solid solutions with various Ce/Zr ratios have been studied as supports for nickel catalysts by Kambolis *et al*. They aimed to study the influence of the binary oxide composition on coke formation resistance and on the textural, structural, and catalytic properties of the nickel catalyst. Results showed that binary CeO_2–ZrO_2 oxides and nickel catalysts supported on these oxides present improved stability under the thermal reductive treatment. The catalysts supported on binary oxides were found much more active than those that were supported on pure ceria. This was attributed to the higher surface density of active sites on the ternary catalysts. In the presence of Zr^{4+}, filamentous carbon was reported to be formed, which was not detected in Ni/CeO_2 spent catalyst. Higher amounts of carbonaceous deposits were accumulated on the nickel catalysts supported on ceria-rich CeO_2–ZrO_2 supports (Kambolis *et al.*, 2010).

Coating metal oxides on the high surface area supports like $MgAl_2O_4$ and alumina which show good activity, stability and coke resistance in DR decreases the final cost. $MgAl_2O_4$ has good basic properties which are suitable for the dry reforming. In their work, Eltejaei *et al*. focused on developing stable Ni (10 wt%) catalysts for CDRM using $MgAl_2O_4$ spinel and high surface area γ-Al_2O_3 as supports with different cerium-zirconium (Ce/Zr atomic ratio= 3) contents (0, 5, 10 and 15 wt%) as promoters. $MgAl_2O_4$ supported catalysts were found to have higher reducibility and stronger basic sites in the presence of $CeZrO_2$ promoters due to higher basicity of $MgAl_2O_4$ compared to γ-Al_2O_3. 5 wt% $CeZrO_2$ promoted Ni/$MgAl_2O_4$ and unpromoted Ni/γ-Al_2O_3 exhibited the highest activity. The different activity levels of the catalysts clearly showed that the catalytic performances of promoted catalysts strongly depended on the nature of support. Moreover, addition of water to feed was found to increase stability and decrease coke formation (Eltejaei *et al*., 2012).

Another study in which Mg was used as a promoter was carried out by K.-M. Kang *et al.* They synthesized Al_2O_3 and MgO–Al_2O_3 supported nickel catalysts with core/shell structures under multi-bubble sonoluminescence (MBSL) conditions and tested them for their CDRM performance. In the tests, 92% conversion was achieved at 800°C with a good thermal stability for the first 150 h time-on-stream. The fixed amounts of carbon deposited on the surface of the catalysts did not influence the activity or thermal stability (Kang *et al.*, 2011).

In their study, Daza *et al*. aimed to evaluate the effect of the Al/Ce ratio on CDRM performances of Ni-Mg-Al-Ce oxides synthesized by the co-precipitation technique. It was reported that the increase in the Al/Ce ratio increased the basicity and the catalytic activity of the catalyst. However, after the reduction of the catalyst, high loads of Ce favored the increase of the particle sizes of Ni^0 and CeO_2. The large particle size decreased the catalytic activity and selectivity, and enabled coke formation. The catalyst with the Al/Ce=24 molar ratio showed the highest conversions and was stable up to 50 h of reaction at 700°C with a CO_2/CH_4= 20/20 (48 L $g^{-1}h^{-1}$) in the feed (Daza *et al*., 2011).

Molybdenum is another promising promoter. L.A. Arkatova studied a novel synthetic approach based on the self-propagating high-temperature synthesis which could be applied

successfully in preparing Ni_3Al. Results indicated that, Ni_3Al and Ni_3Al +5% Mo were very promising catalysts for CDRM. Eventhough Ni sintering occured, Ni_3Al showed high thermal resistance as a support. In addition, it is reported that Mo promoter enhanced the catalytic activity and stability of Ni_3Al catalyst. It was indicated that the reason of the decrease in carbon deposition in the presence of Mo stemmed from the formation of very active and stable Mo_2C phase and Ni–Mo alloy, resulting in reduction of both carbon solubility and dehydrogenation activity during CDRM (Arkatova, 2010).

Li *et al*. investigated the activity, stability and coking resistance property of nickel-based catalysts supported on $BaTiO_3$–Al_2O_3 for dry reforming of methane at low temperatures. Results exhibited that the Ni/$BaTiO_3$ catalyst was prone to coke formation in low temperature dry reforming of methane and this property was attributed to the excessive strong electronic donor intensity of the active nickel component in the Ni/$BaTiO_3$ catalyst as well as the CO disproportionation reaction taking place. Compared with the Ni/$BaTiO_3$ catalyst, it was found that, the synthesized Ni/32.4%$BaTiO_3$–Al_2O_3 catalyst had well reducibility and optimum electronic donor intensity which effectively decreased the coke formation, resulting in higher activity and stability performance (Li *et al.*, 2012).

The modification of Ni-based catalyst by a very small amount of noble metal can result in an inexpensive bimetallic supported system assuring both high activity and low carbon formation (Ozkara-Aydınoglu *et al.*, 2011). Miguel *et al*. aimed to develop a new and effective Ni catalyst modified by a small amount of noble metal in order to obtain relatively cheap supported bimetallic catalysts with an improved catalytic activity and stability for the CDRM. They prepared Pt(0.5%)/Al_2O_3 and Ni(10%)/Al_2O_3 monometalic catalysts and bimetallic Pt(0.5%)Ni(10%)/Al_2O_3 catalyst. It was observed that for the Pt(0.5%)/Al_2O_3 catalyst, a significant sintering of the metallic phase occured. On the other hand, the Ni(10%)/Al_2O_3 catalyst showed a high and stable activity. The bimetallic Pt(0.5%)Ni(10%)/Al_2O_3 catalyst also showed a high and constant activity, moreover, the carbon deposition was found lower than that of Ni(10%)/Al_2O_3 catalyst (Miguel *et al.*, 2012).

Ozkara- Aydınoglu *et al.* studied CDRM over a series of Pt-Ni bimetallic catalysts supported on δ-Al_2O_3. XRD, XPS, TGA/DTA and SEM-EDS were used for the

characterization of selected catalyst samples, before and after reaction. The activity results exhibited that the catalytic performance of bimetallic Pt-Ni samples strongly depended on the metal loadings and Ni/Pt loading ratio. Among all the catalysts, 0.3Pt-10Ni catalyst with the lowest Ni/Pt ratio exhibited the highest catalytic activity and stability. Moreover, low Ni/Pt molar loading ratio of 0.3% Pt-10% Ni/Al_2O_3 sample led to relatively easy reduction of nickel oxide species and to smaller nano-sized nickel particles yielding a better dispersion (Ozkara-Aydınoglu *et al.*, 2011).

Steinhauer *et al.* investigated the performance of Ni-Pd bimetallic supported catalysts at 500, 600 and 700°C under atmospheric pressure with a CH_4 to CO_2 feed ratio of 1. Fresh, spent and regenerated catalysts were characterized by N_2 adsorption, XRD, ICP, XPS and TEM. It was found that the catalytic activity of the studied Ni-Pd catalysts depended strongly on the support used and decreased in the following order: ZrO_2-La_2O_3, La_2O_3 > ZrO_2 > SiO_2 > Al_2O_3 > TiO_2. In addition, the bimetallic catalysts were found more active than catalysts containing Ni or Pd alone. It was indicated that the coke formation increased with increasing Ni/Pd ratio. A Ni to Pd ratio of 4 for a total metal loading of 7.5 wt% gave the best result. Moreover, 600°C was found to be most favorable calcination temperature. Best conversions were obtained using a 7.5 wt% Ni-Pd (80:20) ZrO_2-La_2O_3 supported catalyst at a reaction temperature of 700°C (Steinhauer *et al.*, 2009).

In their work, Ocsachoque *et al.* aimed to clarify the role of CeO_2 addition in Rh–Ni bimetallic catalysts supported on α-Al_2O_3, on the activity, stability and deactivation by carbon deposition during CDRM. Series of Ni and Rh–Ni catalysts supported on Al_2O_3 with CeO_2 with 3-5 wt% Ce loadings were studied. The optimum reaction temperature was found as 650–750°C and the catalyst with 3 wt% Ce loading showed a higher activity and more resistance to carbon formation. It would be associated with the higher dispersion of the active phase (Ocsachoque *et al.*, 2011).

Cobalt is another transition metal which is widely used in the development of novel dry reforming catalysts. Omata *et al.* investigated the catalytic performance of Co–SrO catalyst for CDRM at 1 MPa and 800°C. The catalyst prepared by oxalate co-precipitation method or citric acid method showed a steady activity. In addition, cobalt supported on strontium carbonate prepared by impregnation method (Co/$SrCO_3$) showed a comparable

activity with high tolerance to oxidative atmosphere under reaction conditions (Omata *et al.*, 2004).

The same group also investigated CDRM performance with cobalt–magnesia (Co–MgO) catalyst which was prepared by oxalate co-precipitation method. Co–MgO (7 mol% Co) performed a stable activity at 1 MPa, 800°C and high space velocity of 400000 cm^3h-1g-1. However, the reactor was plugged during the reforming reaction with 10 mol% Co–MgO and the activity of Co–MgO with Co content less than 6 mol% gradually decreased by the oxidation of cobalt species. Results showed that well-balanced cobalt content or hydrogen co-feed is essential for high and stable activity (Omata *et al.*, 2004).

Ruckenstein and Wang studied MgO supported Co catalyst. The effect of CaO, SrO, BaO, γ-Al_2O_3 and SiO_2 were also investigated as supports for Co-based CDRM catalysts. It was found out that MgO showed the highest activity and stability with 93% CO and 90% H_2 yields at high space velocity (60000 ml $g^{-1}h^{-1}$) among all, and the performance of the catalyst was the same during 50 h time-on-stream. Although γ-Al_2O_3 gave a high CO yield at the beginning, it rapidly decayed. The catalysts prepared with other supports exhibited low CO yields, and CaO and SiO_2 also have low stabilities. Formation of solid solution of CoO and MgO, which was identified by XRD, enhances the resistance to carbon deposition and sintering. As the oxygen atoms are shared by both Mg and Co in the solution, the strong interaction with Mg makes the solid solution less reducible than pure CoO. Small clusters of metallic Co are generated and these clusters are more stable to sintering than the usual ones. For these reasons, this catalyst exhibits high stability. As a result, the Co/MgO catalyst provided a high and stable activity for the CDRM (Ruckenstein *et al*., 2000).

In their work, S. Ozkara-Aydınoglu and A.E. Aksoylu aimed to design Co-based CDRM catalysts supported on zirconia to improve the performance and coke resistance through the addition of metal additives, namely lanthanum, cerium, manganese, potassium and magnesium. In order to obtain information on the dispersion of metals on the catalyst surface, SEM and energy dispersive X-ray tests were performed. To detect the formation of different Co-X/ZrO_2 crystalline phases led by various modifiers, XRD analyses were also conducted. Moreover, the amount and type of deposited carbon on the surface of the

used catalysts were identified by thermogravimetric/differential thermal analyses (TGA/DTA), and SEM measurements as well. Results showed that although it had high initial activity, monometallic Co/ZrO_2 suffered from severe carbon deposition and La-modified catalyst displayed moderate but stable activity without coke deposition. Among all the catalysts, Ce doped Co/ZrO_2 exhibited the highest activity and had a very limited activity loss in time-on-stream tests (Ozkara-Aydınoglu *et al.*, 2010).

Wang *et al*. prepared Co-incorporated $Ce_{1-x}Zr_xO_2$ catalysts by co-precipitation for carbon dioxide reforming of methane in order to optimize the performances of Co-Ce-Zr-O_x catalysts. The prepared catalysts were characterized by various physico-chemical characterization techniques including TPR, X-ray diffraction, N_2 adsorption at low temperature, XPS and CO_2-TPSR. Among those catalysts for which the ratio of Ce to Zr were varied, the Co-$Ce_{0.8}Zr_{0.2}O_2$ sample containing 16% CoO exhibited a higher catalytic activity and it maintained its activity without significant loss for 60 h. The CO_2 conversion over this catalyst was 75% while the CH_4 conversion was 67% under the conditions of 750°C, 0.1 MPa, 36000 $ml/h^{-1}\cdot gcat^{-1}$, and CO_2/CH_4 molar feed ratio of 1:1. The cubic $Ce_{0.8}Zr_{0.2}O_2$ facilitated a higher dispersion and a higher reducibility of the cobalt component, and the apparent CDRM activation energy for Co-$Ce_{0.8}Zr_{0.2}O_2$ sample was 49.1 kJ/mol (Wang *et al.*, 2010).

Mn doping to Co–Ce–Zr–O_x catalysts remarkably enhanced the catalytic activity and stability of the catalyst. The highest catalytic activity and long-term stability was obtained when the molar ratio of Mn/(Ce+Zr+Mn) was 10%. The improved catalytic behavior was closely related to the surface oxygen species and oxygen mobility. In comparison with that of Co-Ce-Zr-O_x catalyst, the migration of bulk lattice oxygen species became easier, and the content of surface oxygen species was higher for the Mn-doped nanocrystalline Co-Ce-Zr-O_x samples. Temperature-programmed hydrogenation (TPH) characterization showed that the surface coke species could be easily oxidized into CO_x for the Mn-doped nano cobalt-composite catalyst due to the higher amount of mobile oxygen. The Mn incorporation promoted the dispersion of the nano-sized CoO_x crystallites. In comparison with the impregnated samples, CoO_x species dispersed better in the co-precipitated catalysts (Wang *et al.*, 2011).

In their study, Ruckenstein *et al*. investigated the reaction behavior and carbon deposition during CDRM over the γ-Al_2O_3- supported Co catalysts using different Co loadings (between 2 and 20 wt%) and calcination temperatures (500 or 1000°C). It was found that the stability of Co/γ-Al_2O_3 catalysts was strongly dependent on the Co loading and calcination temperature. Stable activities have been achieved for the catalysts with 6 wt% loadings which are calcined at 500°C and the ones with 9 wt% loadings calcined at 1000°C. However, over the catalysts with high Co loadings (>12 wt%), notable amounts of carbon were accumulated during reforming, and deactivation was observed. Moreover, severe deactivation was also noted over the 2 wt% catalysts, both when carbon deposition occurred over the ones which are calcined at 500°C or absent on the catalysts having 1000°C calcination temperature. In the latter case, the oxidation of the metallic sites was responsible for the deactivation. Hence, there were two different deactivation mechanisms, namely, carbon deposition and oxidation of metallic sites. The activities were stable when a balance between carbon formation and its oxidation could be achieved (Ruckenstein *et al*., 2002).

In the study by Lee *et al*. CDRM was performed over Co–Ru–Zr catalyst prepared on different supports (SiO_2, δ-Al_2O_3 and MgO) in order to analyze deactivation. The characteristics of the catalysts, before and after the reaction, were investigated employing BET, XRD, TPR, TGA-DTA and TEM. Among the 0–0.6 wt% Ru containing Co–Ru–Zr catalysts, 0.4 wt% Ru loaded one showed the highest activity due to its smallest crystallite size. This result showed that dispersion of cobalt was affected by Ru amount. In addition, optimum calcination temperature was found as 400°C and catalysts calcined above 600°C were reported to exhibit diminishing activities due to the strong bonds formed between metal and supports (Lee *et al*., 2013).

J. Cheng and W. Huang studied the performance of a series of Co-Mo and Ni–Mo bimetallic carbide catalysts with different Me/Mo (Me= Co, Ni) molar loading ratios. They used X-ray diffraction, FTIR, XPS and N_2 adsorption to find out the relationships between catalytic performance, phase structure and surface properties. Results showed that the addition of a suitable amount of nickel or cobalt to molybdenum oxide enhanced the activity and stability of the synthesized molybdenum carbide catalyst. It was reported that this improvement appeared to be associated with the formation of the Co-Mo and Ni–Mo

carbide phases. The results revealed that optimum Co/Mo and Ni/Mo loading ratios were 0.4 and 0.2, respectively. On the other hand, the authors also reported that some cobalt or nickel atoms existed in the metallic form for higher metal to Mo molar loading ratios and this resulted in decrease of structural and electronic promoting effects (Cheng *et al*., 2010).

Among non-noble metals, the combination of cobalt and nickel supported on ZrO_2 and Al_2O_3 are known to show an enhancement of catalytic performance towards the methane reforming reaction, ascribed to a synergic effect due to the formation of Co-Ni alloy (Luisetto *et al.*, 2012). Luisetto *et al*. prepared Co-Ni/CeO_2 catalyst and compared its CDRM performance with Ni/CeO_2 and Co/CeO_2 systems aiming to investigate the effect of the supported metal on the catalytic activity and carbon deposition. Results exhibited that the Co-Ni/CeO_2 catalyst was more active and more selective than the Co/CeO_2 and Ni/CeO_2 monometallic catalysts for CDRM. Both cobalt-containing catalysts, Co-Ni/CeO_2 and Co/CeO_2, showed a higher resistance to carbon deposition than Ni/CeO_2. Bimetallic Co-Ni/CeO_2 was found beneficial because it integrated the high activity of nickel with the high resistance of cobalt towards carbon deposition, behaving as a highly active, selective and thermally stable catalyst for the syngas production by methane dry reforming (Luisetto *et al.*, 2012).

In their work, Alonso *et al*. studied CDRM over Ni, Co and Ni–Co alumina supported catalysts (9 wt% nominal metal content) to determine the optimum catalyst formulation for the reaction. The catalysts with the highest cobalt content, Co (9 wt%) and NiCo (1–8 wt%), were found the most active and stable among the studied ones, however they produced a large amount of carbon. It was explained that the higher activity exhibited by cobalt rich catalysts could be due to the higher activity of this metal for methane decomposition. As a result, it was reported that Co rich catalysts had good catalytic properties but improvements were needed to overcome coke deposition (San-Jose´-Alonso *et al*., 2009).

2.2. Kinetics of CO_2 Reforming of CH_4

Despite the fact that literature concerned with CDRM has focused on activity extensively, less emphasis has been given to fundamental understanding of the reaction

kinetics (Souza *et al*., 2001). However, it is essential to identify the reaction mechanism and the rate determining steps in order to develop a high performance catalyst (Cui *et al.*, 2007).

2.2.1. Suggested Mechanisms and Rate Expressions

In practice, a heterogeneous catalyst may have a distribution of catalytic active sites with different intrinsic activation barriers for the chemical reaction of interest (Bradford and Vannice, 1999). Some of reported activation energies for CDRM are given in Table 2.1. The analysis of the reported values reveals that the activation barrier for CH_4 consumption is higher than that for CO_2 consumption and the activation energy for H_2 is greater than the activation energy of CO.

Table 2.1. Apparent activation energies (E_{app}) over Ni, Pt & Co catalysts.

Catalyst	E_{app} (kcal/mol)				Reference
	CH_4	CO_2	CO	H_2	
Pt/ZrO_2	15	14	15	-	Bradford and Vannice, 1998
Pt/ZrO_2	24.0	20.0	21.6	34.0	Bradford and Vannice, 1998
Pt/ZrO_2	18.4	15.0	15.0	16.8	Souza *et al.*, 2001
Ni/ZrO_2	14	10	12	-	Bradford and Vannice, 1998
$Ni\text{-}K/CeO_2\text{-}Al_2O_3$	11.0	11.0	11.3	12.9	Nandini *et al.*, 2006
Co/Al_2O_3	-	-	14	-	Bradford and Vannice, 1998
Co/C	11.0	9.0	9.0	11.0	Guerrero-Ruiz *et al.*, 1994
Co/SiO_2	10.0	8.0	9.0	11.0	Guerrero-Ruiz *et al.*, 1994
$Co/MgO/SiO_2$	12.0	9.0	10.0	13.0	Guerrero-Ruiz *et al.*, 1994
Co/MgO/C	14	11	16	-	Guerrero-Ruiz *et al.*, 1994
Co/SiO_2	10	8	9	11	Guerrero-Ruiz *et al.*, 1994

It is well known that the overall reaction order is significantly affected by active metal and support. This indicates that the reaction mechanism differs according to the type of the catalysts used.

In their work, Y. Cui *et al*. studied the effect of temperature on the CDRM mechanism. They investigated the mechanism and the rate-determining steps over the typical Ni/α-Al_2O_3 catalyst. In the experimental work, steady-state and transient kinetic methods with a temperature range of 550–750°C was used. The activation energies of the reforming reactions, together with the reaction orders of CH_4, CO_2, H_2, and CO, exhibited that the reaction mechanism can be divided into three regions: 550-575°C, 575-650°C, and 650-750°C. In addition, the reaction rate was found out constant in the low and high temperature ranges but was varied in the middle region. Moreoever, the CH_4 dissociation into CH_x species and hydrogen species reached equilibrium state above 650°C. The surface oxygen species originating from CO_2 became removable and reacted with CH_x species above 575°C. Above 650°C, CH_4 dissociation was found faster than the reaction rate of CH_x with CO_2 which led to the durative carbon deposition on the catalyst. CO competed with CH_4 on the Ni active sites and inhibited the dry reforming below 650°C; and CO was desorbed rapidly above 650°C. The formation of hydrogen is a rapid or equilibrium step in the reforming reaction. Therefore, the rate determining step was CH_4 dissociation, and CO desorption also restrained the reforming reaction in 550-575°C temperature range. On the other hand, in the range of 650-750°C, the reaction between CH_x and CO_2 became the rate determining step. The results showed that the change of reaction temperature influenced the reforming mechanism through varying the reaction steps (Cui *et al.*, 2007).

Wang *et al*. used Density Functional Theory calculations utilizing B3LYP basis set and CCSD(T) method to investigate the thermal CO_2 reforming of CH_4. It was found that the first step was the CH_4 dissociation into CH_3 and H radicals for the chain initiation reaction. The continuing reforming reaction was the reaction of CH_3 with CO_2, which led the formation of CH_3O radical and one of the principal products, CO. Further degradation of CH_3O via one or two step gave also CO as product. The produced hydrogen radical from the whole processes led another principal product, H_2. The CH_xO reaction path was more favored than the CH_x alternative (Wang *et al*., 2004).

Laosiripojana *et al*. studied the reactivity toward dry reforming and the resistance to carbon formation over CeO_2 doped Ni/Al_2O_3 and compared to conventional Ni/Al_2O_3 at the temperature range of 800-900°C. The intrinsic reaction kinetics of 8% CeO_2 doped Ni/Al_2O_3 was studied by varying inlet CH_4 and CO_2 concentrations, and by adding H_2 and

CO to the system at different temperatures. It was found that the dry reforming rate increased with increasing methane partial pressure and the operating temperature. The reaction orders in methane were always closed to 1.0 in all conditions. Carbon dioxide also presented weak positive impact on the methane conversion, while carbon monoxide and hydrogen addition inhibited the reforming rate. Regarding to the experiments conducted, rate equation with constants was observed as:

$$-r_{CH_4} = \frac{k(T)\left(P_{CH_4}\right)^n\left(P_{CO_2}\right)^m}{1 + K_1(T)P_{CO}^a + K_2(T)P_{H_2}^a} \quad (2.8)$$

where P_i is the partial pressure of chemical component i. Constants were found as n=1.0, m=0.5, a=0.4, b=0.5. k(T) increased from 649.0 mol $kg^{-1}h^{-1}atm^{-1.5}$ at 825°C to 954.3 mol $kg^{-1}h^{-1}atm^{-1.5}$ at 900°C and $K_1(T)$ and $K_2(T)$ were in the range of 1.68-4.43 $atm^{-0.4}$ and 0.93-3.94 $atm^{-0.5}$, respectively. Moreover, the apparent activation energy achieved by the Arrhenius plots was approximately 150 kJ/mol (Laosiripojana *et al.*, 2005).

Laosiripojana *et al*. also reported that a high surface area CeO_2 with the surfactant assistance had better reforming reactivity and carbon deposition resistance due to its high redox property. The CH_4–CO_2 reforming over CeO_2 and CeO_2-containing materials could undergo the following cycle:

$$CeO_2 + nCH_4 \rightarrow CeO_{2-n} + nCO + 2nH_2 \quad (2.9)$$

$$CeO_2 + nH_2 \rightarrow CeO_{2-n} + nH_2O \quad (2.10)$$

$$CeO_{2-n} + nCO_2 \rightarrow CeO_2 + nCO \quad (2.11)$$

The reaction between CH_4 and the surface lattice oxygen species of CeO_2 was suggested as the controlling step. The activation energies and reforming rates under the same methane concentration for CeO_2 toward dry reforming were almost equal to the steam reforming data in the literature. These results suggested similar reaction mechanisms for the steam reforming and the dry reforming over CeO_2; i.e., the dry reforming rate was governed by the slow reaction of adsorbed methane, or surface hydrocarbon species, with oxygen in

CeO_2, and a rapid gas–solid reaction between CO_2 and CeO_2 to replenish the oxygen Laosiripojana *et al*, 2005).

Nandini *et al*. studied the effect of reaction parameters on the catalytic activity of Ni-K/CeO_2-Al_2O_3 catalyst for CDRM. The kinetic behavior of the Ni-K/CeO_2-Al_2O_3 catalyst in the reforming reaction was investigated as functions of temperature and partial pressures of CH_4 and CO_2. The apparent activation energy for CH_4 and CO_2 consumption, and H_2 and CO production were 46.1 ± 2.5, 46.2 ± 2.4, 54.0 ± 2.6 and 47.4 ± 1.7 kJ/mol for the temperature range of 600-800°C, respectively. It was found that an increase of the H_2 partial pressure leads to a continuous enhancement of the CO formation rate due to water–gas shift reaction. Methane consumption rate was strongly affected by the partial pressure of methane. Variation of the CO_2 partial pressure had also a strong influence on methane consumption rate at low partial pressures of 0-0.1 atm, while methane consumption was insensitive to CO_2 partial pressure at high pressures. With respect to experimental data and literature data the following generalized reaction mechanism was proposed:

$$CH_4 + * \overset{k_1}{\rightarrow} CH_x^* + \left(\frac{4-x}{2}\right) H_2 \tag{2.12}$$

$$2\left[CO_2 + * \overset{K_2}{\leftrightarrow} CO_2^*\right] \tag{2.13}$$

$$H_2 + 2^* \overset{K_3}{\leftrightarrow} 2H^* \tag{2.14}$$

$$2\left[CO_2^* + H^* \overset{K_4}{\leftrightarrow} CO^* + OH^*\right] \tag{2.15}$$

$$OH^* + H^* \overset{K_5}{\leftrightarrow} H_2O + 2^* \tag{2.16}$$

$$CH_x^* + OH^* \overset{K_6}{\leftrightarrow} CH_xO^* + H^* \tag{2.17}$$

$$CH_xO^* \overset{k_7}{\leftrightarrow} CO^* + \left(\frac{x}{2}\right) H_2 \tag{2.18}$$

$$3\left[CO^* \overset{K_8}{\leftrightarrow} CO + *\right] \tag{2.19}$$

which corresponds to the overall reaction stoichiometry:

$$CH_4 + 2CO_2 \rightarrow H_2 + H_2O + 3CO \tag{2.20}$$

The apparent activation energy barrier for hydrogen formation was greater than that for the formation of carbon monoxide (54 kJ/mol and 47.4 kJ/mol, respectively) indicating that Eqs. 2.12 and 2.18 involving the formation of H_2 are likely to be the rate limiting steps of the CH_4/CO_2 reaction over the Ni-K/CeO_2-Al_2O_3 catalyst. Based on the mechanism, a kinetic model was developed (Nandini *et al.*, 2006).

$$r_{CH_4} = \frac{k_{1L} p_{CH_4}}{\left[\left(\frac{k_{1L}\, p_{CH_4}\, p_{CO}}{k_{7L}} K_a\, p_{CO_2}\right) + \left(\frac{K_b\, p_{CO_2}\, p_{H_2}^{\frac{1}{2}}}{p_{CO}}\right) + \left(\frac{k_{1L}\, p_{CH_4}}{k_{7L}}\right) + 1\right]} \tag{2.21}$$

and $r_{CH_4} = ck_{1L}p_{CH_4}$ for $p_{CO_2} \geq 0.75$ atm where k_{1L}=1.0221e-3 g mol/g_{cat} s atm, k_{7L}=3.01e-3 g mol/g_{cat}, K_a=6.8e-2 atm^{-2}, K_b=0.64 $atm^{-2.5}$ and c=0.66 at 923 K.

Akpan *et al.* carried out reactions in order to develop a kinetic model of CDRM over Ni/CeO_2–ZrO_2 catalyst. They proposed a mechanism for CDRM, based on the experimental and relevant literature data.

$$CH_4 + 2S \overset{k_1, k_{-1}}{\longleftrightarrow} CH_{3(s)} + H_{(s)} \tag{2.22}$$

$$CH_{3(s)} + S \overset{k_1, k_{-1}}{\longleftrightarrow} CH_{2(s)} + H_{(s)} \tag{2.23}$$

$$CH_{2(s)} + S \overset{k_1, k_{-1}}{\longleftrightarrow} CH_{(s)} + H_{(s)} \tag{2.24}$$

$$CH_{(s)} + S \overset{k_1, k_{-1}}{\longleftrightarrow} C_s + H_{(s)} \tag{2.25}$$

Combining Eqs. 2.22 and 2.25 gave Eq. 2.26 which represents the CH_4 adsorption and dissociation to a CH_x fragment or distribution of CH_x fragments.

$$CH_4 + 5S \overset{k_1,k_{-1}}{\longleftrightarrow} C_s + 4H_{(s)} \tag{2.26}$$

Eq. 2.27 represents formation of solid carbon which was produced via CH_4 dissociation.

$$C_{(s)} + O_x \overset{k_2,k_{-2}}{\longleftrightarrow} CO + O_{x-1} + S \tag{2.27}$$

CO_2 always reacted with the reduced site of the catalyst (Laosiripojana and Assabumrungrat, 2005a). So, Eq. 2.28 represents the oxidation of the reduced CeO_2–ZrO_2 sites (O_{x-1}) by reacting with CO_2 molecules.

$$CO_{(2)} + O_{(x-1)} \overset{k_3,k_{-3}}{\longleftrightarrow} CO + O_x \tag{2.28}$$

The high reducibility and oxygen storage capacity of the CeO_2–ZrO_2 support provide highly mobile oxygen species via a redox cycle. That made reaction steps given in Eq. 2.27 and 2.28 to readily proceed forward. Similarly, the formation of water was also explained in Eq. 2.30 through reverse-water-gas-shift reaction generally present in the system.

$$4H_{(s)} \overset{k_4,k_{-4}}{\longleftrightarrow} 2H_2 + 4S \tag{2.29}$$

$$H_2 + O_x \overset{k_5,k_{-5}}{\longleftrightarrow} O_{(x-1)} + H_2O \tag{2.30}$$

where (S) and O_x represent unoccupied active sites and lattice oxygen on $Ce_{0.6}Zr_{0.4}O_2$ surface, respectively. The power rate model:

$$r_A = k_0 e^{-E/RT} N_{CH_4}^n \tag{2.31}$$

was used as a reference for assessing the accuracy of empirical kinetic data where r_A=kg-methane/kg-cat h; k_0= preexponential factor; E= activation energy, J/mol; R= gas constant, 8.314 J/mol; T=absolute temperature, K; N_{CH4}= CH_4 flow rate, mol/h and n=reaction order.

Reaction steps given in Eq. 2.26- 2.29 based on Eley-Rideal (ER) formulation were used in the derivation of mechanism based rate expressions representing four possible rate determining steps (RDS).

Model #1: (RDS=Eq. 2.26)

$$r_A = \frac{k_0 e^{-E/RT}\left(N_{CH_4} - \frac{N_{CO}^2 N_{H_2}^2}{K_p N_{CO_2}}\right)}{\left(1 + K_A \frac{N_{CO}^2}{N_{CO_2}} + K_B N_{H_2}^{1/2}\right)^5} \qquad (2.32)$$

Model #2: (RDS=Eq. 2.27)

$$r_A = \frac{k_0 e^{-E/RT}\left(\frac{N_{CH_4}}{N_{H_2}^2} - \frac{N_{CO}^2}{K_p N_{CO_2}}\right)}{\left(1 + K_A \frac{N_{CO}^2}{N_{CO_2}} + K_B N_{H_2}^{1/2}\right)} \qquad (2.33)$$

Model #3: (RDS=Eq. 2.28)

$$r_A = \quad k_0 e^{-E/RT}\left(\frac{N_{CH_4} N_{CO_2}}{N_{CO} N_{H_2}^2} - \frac{N_{CO}}{K_p}\right) \qquad (2.34)$$

Model #4: (RDS=Eq. 2.29)

$$r_A = \frac{k_0 e^{-E/RT}\left(\frac{N_{CH_4} N_{CO_2}}{N_{CO}^2} - \frac{N_{H_2}^2}{K_p}\right)}{\left(1 + K_A \frac{N_{CO}^2}{N_{CO_2}} + K_B N_{H_2}^{1/2}\right)^4} \qquad (2.35)$$

where N represents flow rates, mol/h; K_A is adsorption constant and K_p is the equilibrium constant at T_0 (Akpan *et al.*, 2008).

In the same study, Akpan *et al*. also used two-dimensional pseudo-homogeneous numerical model including material and energy balance equations for reactor modelling. The experiments were carried out at atmospheric pressure and temperatures of 863, 823 and 973 K. The model was developed based on the the Eley–Rideal (ER) formulation and the methane dissociative adsorption was taken to be the rate-determining step. The reactor model including the axial dispersion term was found to be the best model. Thus, it was recommended to use the axial dispersion terms in the mass and energy balance equations in order to obtain befitting results (Akpan *et al.*, 2008).

3. EXPERIMENTAL WORK

3.1. Materials

3.1.1. Chemicals

All the chemicals used for catalyst preparation are presented in Table 3.1.

Table 3.1. Chemicals used in catalyst preparation (all specifications: research grade).

Chemicals	Formula	Source	Molecular Weight (g/mol)
Cerium (III) nitrate hexahydrate	$Ce(NO_3)_3.6H_2O$	Merck	434.23
Cobalt (II) nitrate hexahydrate	$Co(NO_3)_2.6H_2O$	BDH	290.93
Aluminum oxide	Al_2O_3	Alfa Aesar	101.96
Zirconium oxide	ZrO_2	Alfa Aesar	123.22

3.1.2. Gases and Liquids

The gases used in this research were supplied by BOS A.Ş. and Linde Group. The specifications and applications of the liquids and gases in this study are listed in Tables 3.2 and 3.3.

Table 3.2. Specification and application of the liquid used.

Liquid	Specification	Application
Water	De-ionized	Aqueous solutions, Reactant

Table 3.3. Specifications and application areas of the gases used.

Gas/Standard	Specification	Application
Argon	99.998%	Inert, GC Carrier Gas
Carbon dioxide	99.995%	Reactant, GC calibration
Carbon monoxide	99.999%	GC calibration
Dry air	99.998%	Calcination, GC 6-way pneumatic valve
Hydrogen	99.990%	Reduction, GC calibration
Methane	99.500%	Reactant, GC calibration
Nitrogen	99.99%	Inert, GC calibration

3.2. Experimental Systems

There are four main groups of experimental systems used in this study:

(i) Catalyst Preparation System: This is the system used for preparing the catalyst by incipient-to-wetness impregnation technique.

(ii) Catalyst Characterization Systems: These systems include different analytical and spectroscopic techniques which were used to characterize the physical, microstructural and electronic properties of the catalyst samples prepared and to examine any carbonaceous deposits produced after reaction test.

(iii) Catalytic Reaction System: The catalytic reaction system was used for determining the catalytic activity, selectivity, stability and for measuring reaction kinetics. It is a continuous flow microreactor system including mass flow controllers, a temperature controlled oven and a reaction chamber.

(iv) Product Analysis System: The quantitative determination of species composition both in the reactor effluent and feed stream was conducted by a gas chromatograph connected on-line to the microreactor flow system.

3.2.1. Catalyst Preparation System

The system used for preparing catalysts by incipient-to-wetness impregnation technique (Figure 3.1) included a Retsch UR1 ultrasonic mixer, a vacuum pump, a Buchner flask and a MasterFlex computerized-drive peristaltic pump.

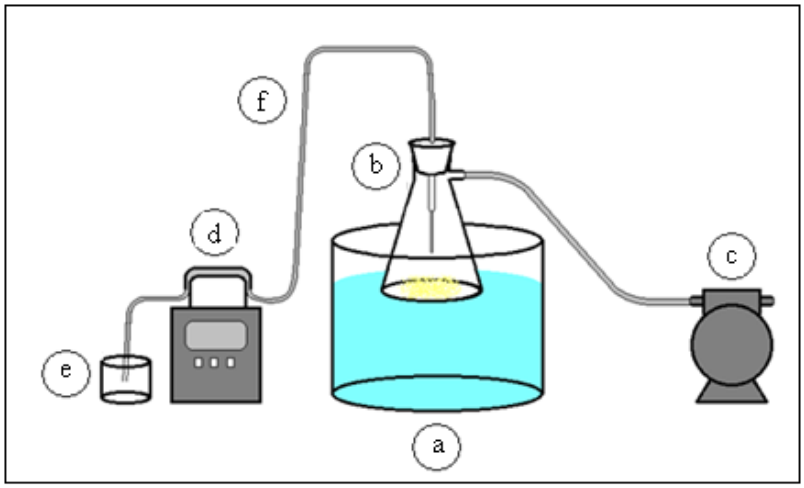

Figure 3.1. Schematic diagram of the impregnation system
(a) Ultrasonic mixer, (b) Büchner flask, (c) Vacuum pump, (d) Peristaltic pump, (e) Reactant storage tank and (f) Silicone tubing.

3.2.2. Catalyst Characterization Systems

3.2.2.1. X-Ray Diffraction (XRD). To identify the crystalline phases of the catalyst samples and their particle sizes a Rigaku D/MAX-Ultima+/PC X-ray diffraction equipment having an X-ray generator with Cu target and scan speed of 2°/min was used. The experiments were performed at Advanced Technologies Research and Development Center of Bogazici University.

3.2.2.2. Scanning Electron Microscopy (SEM). Freshly reduced and spent Co-Ce/ δ-Al_2O_3 samples were characterized by SEM and SEM-EDX (Energy Dispersive X-Ray)

aiming to analyse their microstructure, metal dispersion and coke formation on their surface during CDRM performance tests. The textural properties and metal dispersion of freshly reduced Co-Ce/ZrO_2 samples were also analyzed by SEM-EDX. Philips XL 30 ESEM-FEG system was used with a maximum resolution of 2 nm. The experiments were performed at Advanced Technologies Research and Development Center of Boğaziçi University.

3.2.3. Catalytic Reaction System for CDRM Reaction

The catalytic reaction system was designed and constructed in the Catalysis and Reaction Engineering Laboratory of Chemical Engineering Department, Boğaziçi University, and involves feed, reaction and product analysis sections.

Feed preparation section consists of mass flow control systems, 1/4", 1/8" and 1/16" stainless steel tubes and fittings for feeding gaseous species, i.e. methane, carbon dioxide, nitrogen, hidrogen, carbon monoxide and dry air. The gases were supplied by pressurized gas cylinders and the flow rates of the gases were controlled by Brooks Instrument mass flow controllers. The flow rate values were adjusted by the Brooks Instrument 0154 series control box for carbon dioxide, nitrogen, hidrogen, carbon monoxide and 0254 series control box for methane and dry air. On-off valves were placed in front of the mass flow controllers to protect them from possible back-pressure fluctuations. To adjust desired feed ratios and evaluate the flow of individual species, each gas was fed from its independent line. The gases were then introduced through a primary mixing zone in order to have the flow of homogenous reactant gas mixture into the reactor. The system configuration enables diverting the flow direction of feed gases to bypass line by using a three way valve before entering the reactor so that the feed composition could be measured by the gas chromatograph.

The reactants, measured and mixed in the feed section, were allowed to flow through the reaction section. This section was composed of a 45 cm × 20 cm × 20 cm furnace controlled by a Eurotherm 3216P programmable temperature controller with ±0.1 K precision connected to a K type sheathed thermocouple and a 12 mm ID, 75 cm long quartz down-flow microreactor. For connecting the quartz reactor to the system from both

ends of the ractor, stainless steel fittings welded to 1/4" stainless steel tubes were designed and constructed. Identical fittings with 12 mm inner diameter, 24 mm outer diameter and 50 mm height prevented any gas leak. Sintered quartz disc, which was welded to the center of the quartz microreactor, was used to hold the catalyst bed in a fixed position. Ceramic glass wool insulations were placed on top and bottom ends of the reactor furnace to prevent heat loss.

The steam produced during reaction was removed by placing two ice cold traps after the reactor to avoid any condensation in the gas chromotograph column.

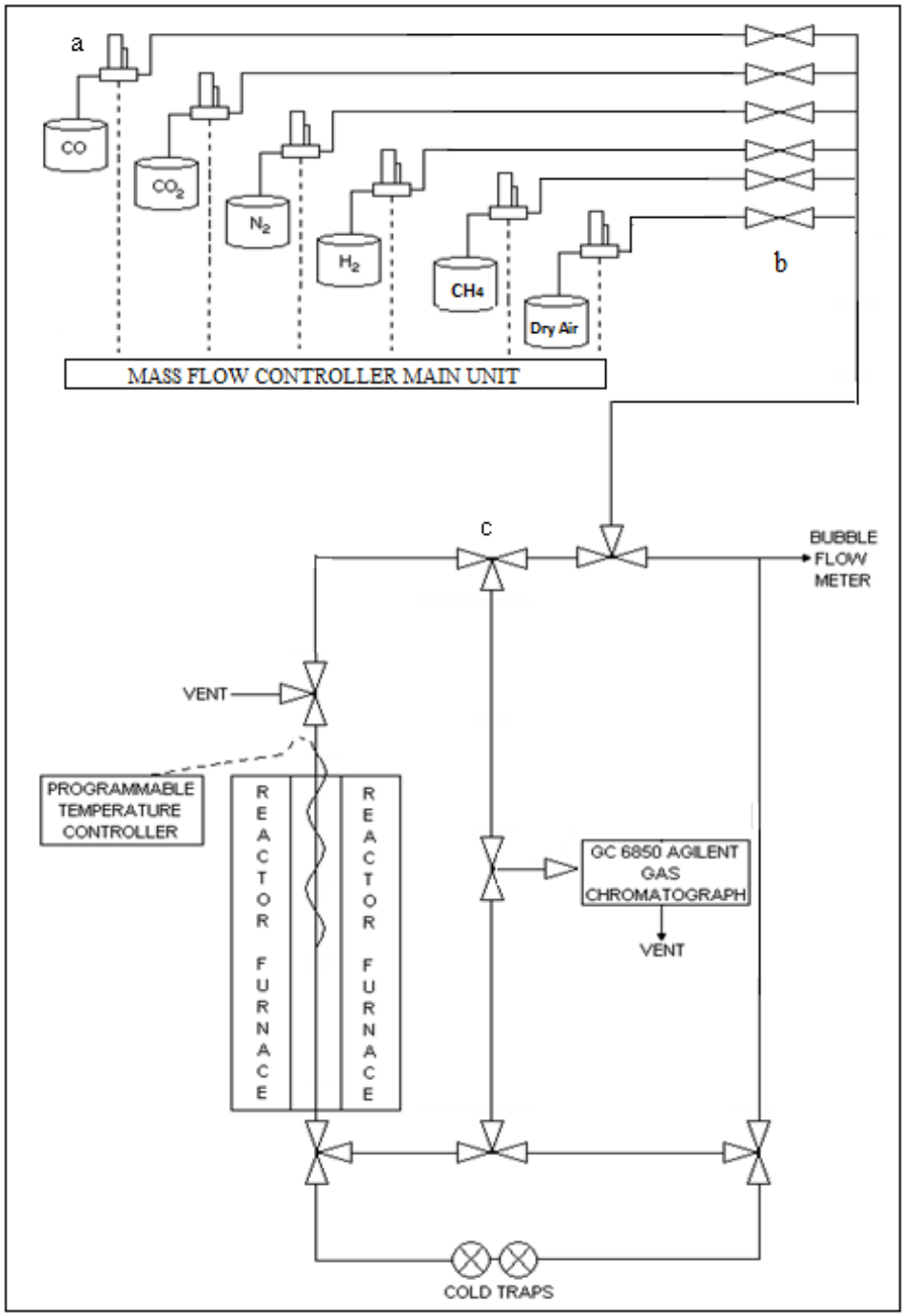

Figure 3.2. Schematic diagram of the microreactor flow system

(a) Mass flow controller, (b) On-off valve, (c) Three-way valve and (d) Mixing zone.

3.2.4. Product Analysis System

Agilent Technologies 6850 gas chromatograph (GC) equipped with a Thermal Conductivity Detector (TCD) and a HayeSep D column was used to detect feed and product stream. Analysis conditions are given in Table 3.4.

Table 3.4. Reactant and product gas analysis conditions.

Gas Chromatograph	Agilent Technologies 6850
Detector type	TCD
Column temperature, °C	50
Inlet temperature, °C	100
Detector temperature, °C	150
Carrier gas	Argon
Carrier gas flow rate, ml/min	20
Column packing material	Hayesep D
Column tubing material	Stainless steel
Column length & ID	3m x 3 mm
Sample loop	1 ml

Before proceeding with the experiments, the gas chromatograph was calibrated by sampling known values of the gases to be analyzed under the conditions given in Table 3.4. Using this procedure, volume versus peak area curves were constructed for each gas and the corresponding calibration factors were determined by linear regression.

3.3. Catalyst Preparation and Pretreatment

In this thesis, two sets of catalysts were prepared:

- 5 wt% Co-2 wt% Ce/δ-Al_2O_3
- 10 wt% Co-2 wt% Ce/ZrO_2

3.3.1. Support Preparation

Due to the endothermic nature of the CDRM, elevated temperatures are required to reach high conversion levels. Therefore, the catalyst supports should not only have high surface areas but also must possess high thermal stabilities to prevent sintering.

3.3.1.1. Alumina. The thermally stable δ-Al_2O_3 support was obtained by drying crushed and sieved (45-60 mesh) γ- Al_2O_3 at 150°C for 2 h and then calcining it at 900°C for 4 h. Although this heat treatment caused a reduction in the BET surface area, from 279 m^2/g to 81.6 m^2/g after calcination, thermal stability of the support was improved.

3.3.1.2. Zirconia. The support was calcined at 800°C for 4 h in muffle furnace prior to the addition of the metals. Although this heat treatment caused a reduction in the BET surface area, from 93 m^2/g to 16 m^2/g, thermal stability of the support was improved.

3.3.2. Preperation of Catalysts

The experimental set-up shown in Figure 3.1 was used for catalyst preparation by the incipient-to-wetness impregnation which consists of three parts:

- Evacuating the support,
- Contacting the support with the precursor solution, and
- Drying.

For incipient wetness impregnation, five grams of support was placed in the Büchner erlen and kept under vacuum both before and during the addition of precursor solutions. A vacuum pump was used to prevent the support from trapped air and to give a uniform distribution of the active component. Before impregnating the solution, the support material was mixed with ultrasonic mixer for 25 min.

In both of the catalysts, impregnation of aqueous precursor solution of cerium (cerium (III) nitrate hexahydrate) was performed first. This was followed by heat treatment

at 500 °C for 4 h in muffle furnace and impregnation of aqeous solution of cobalt (cobalt (II) nitrate hexahydrate). A Masterflex computerized-drive peristaltic pump was used to feed the precursor solution to the vacuum flask at a rate of 5 mL/min via silicone tubing at each impregnation step. The slurry was mixed by an ultrasound mixer during the impregnation in order to maintain uniform distribution of the precursor solutions. After the precursor solution was added, the slurry was ultrasonically mixed for an additional 90 min. The thick slurry obtained was dried at 115 °C overnight after each impregnation procedure.

3.3.3. Catalyst Pretreatment

5 wt% Co-2 wt% Ce/δ-Al_2O_3 catalyst was calcined *in situ* in dry air (30 mL/min) for 4 h at 800°C and subsequently reduced *in situ* in H_2 (50 mL/min) for 2 h at the same temperature. Before calcination, the temperature was raised to 800°C under nitrogen flow (25 mL/min) with 15°C/min. Nitrogen flow was also introduced between calcination and reduction periods for 30 minutes in order to prevent the mixing of dry air and hydrogen. After reduction, the nitrogen flow was adjusted to 5 mL/min and the system was left overnight prior to the reaction tests.

10 wt% Co-2 wt% Ce/ZrO_2 catalyst was calcined *in situ* in dry air (30 mL/min) for 4 h at 500°C and subsequently reduced *in situ* under H_2 flow (50 mL/min) for 2 h at the same temperature. Before calcination, the temperature was raised to 500°C under nitrogen flow (25 mL/min) with 15°C/min increase rate. Nitrogen flow was also introduced between calcination and reduction periods for 30 minutes in order to prevent the mixing of dry air and hydrogen. Then, reaction tests were performed.

3.4. Reaction Tests

3.4.1. Blank Tests

Blank tests were conducted to ensure that the material of construction, quartz disc and the reactor did not interfere with the reaction test outputs. The results indicated that quartz disc and the reactor were inert under the conditions used in the reaction experiments.

3.4.2. CO_2 Reforming of CH_4 over 5 wt% Co-2 wt% Ce/δ-Al_2O_3 catalyst

CDRM performance analysis has been conducted over 5 wt% Co-2 wt% Ce/δ-Al_2O_3 catalysts through the experiments for which temperature, CH_4/CO_2 ratio and space velocity were considered as the parameters. After changing the nitrogen flow from 5 mL/min to 25 mL/min, the furnace temperature was increased with the rate of 15°C/min. Meanwhile, the GC operation procedure was followed. After both the GC and the system temperatures were ready, the reactions were performed at 650°C, 700°C, 800°C with CH_4/CO_2 ratios of 1/2 and 1/1 and space velocities of 10000, 20000 and 30000 mL/h g-catalyst. Data for every 30 minutes up to 4 hour were obtained. Then, data for feed analysis were obtained after waiting for 30 minutes for the feed gases to mix completely in the bypass line. Experiments performed in this study are shown at Table 3.5 in detail.

3.4.3. CO_2 Reforming of CH_4 over 10 wt% Co-2 wt% Ce/ZrO_2 catalyst

The kinetics of the CDRM was studied over 10 wt% Co-2 wt% Ce/ZrO_2 catalyst. In the kinetic tests, CH_4 and CO_2 partial pressures were changed according to an experimental design that allows calculating initial rates for 7 different CH_4/CO_2 feed ratio via using three rate data obtained for different residence times, W/F, for each CH_4/CO_2 feed ratio.

All of the reactions were performed under differential conditions at atmospheric pressure at 600°C using 12 mg of catalyst. In order to obtain intrinsic reaction rates, the total flow rates were adjusted between 100-150 mL/min. In this way, external and internal heat/mass transfer effects could be minimized and the conversions could be kept in the range of 5-25 per cent, which were far away from the corresponding thermodynamic equilibrium.

The partial pressure dependencies were determined by maintaining a constant partial pressure of 0.08 atm of one reactant and varying the pressure of the other reactant between 0.02 and 0.08 atm. Nitrogen was adjusted to maintain the pressure close to atmospheric and the total flow constant. The various gas feed compositions used are listed in Table 3.6.

To determine the apparent activation energies, the reforming reaction was carried out with a feed composition of CH_4:CO_2 = 1:1 over a temperature range of 580- 620°C Details are listed in Table 3.7.

The effect of H_2 and CO addition was studied at a total flow of 100 mL/min with 0.08 atm partial pressure of the two reactants, while the inlet partial pressures of H_2 or CO were changed from 0 to 0.075 atm. The various gas feed compositions used are listed in Table 3.8 and 3.9.

Table 3.5. Summary of the experimental conditions used for the performance tests over 5 wt% Co-2 wt% Ce/δ-Al_2O_3 catalyst.

Experiment No	Space Velocity (mL/h g-cat)	Catalyst weight (mg)	CH_4/CO_2 Ratio	Reaction Temperature (°C)
1	20000	50	1/2	650
2	20000	50	1/2	700
3	20000	50	1/2	800
4	20000	50	1/1	650
5	20000	50	1/1	700
6	20000	50	1/1	800
7	10000	100	1/1	700
8	30000	30	1/1	700

Table 3.6. Summary of the experimental conditions used for determining the initial rates over 10 wt% Co-2 wt% Ce/ZrO_2 catalyst.

Experiment No	CH_4/CO_2	Total Flow (ml/min)	Space Velocity (mL/h.gcat)	Partial Pressures (atm)		Temperature (°C)
				CH_4	CO_2	
1	0.25	100	500,000	0.02	0.08	600
2	0.25	120	600,000	0.02	0.08	600
3	0.25	150	750,000	0.02	0.08	600
4	0.5	100	500,000	0.04	0.08	600
5	0.5	120	600,000	0.04	0.08	600
6	0.5	150	750,000	0.04	0.08	600
7	0.75	100	500,000	0.06	0.08	600
8	0.75	120	600,000	0.06	0.08	600
9	0.75	150	750,000	0.06	0.08	600
10	1.00	100	500,000	0.08	0.08	600
11	1.00	120	600,000	0.08	0.08	600
12	1.00	150	750,000	0.08	0.08	600
13	1.33	100	500,000	0.08	0.06	600
14	1.33	120	600,000	0.08	0.06	600
15	1.33	150	750,000	0.08	0.06	600
16	2.00	100	500,000	0.08	0.04	600
17	2.00	120	600,000	0.08	0.04	600
18	2.00	150	750,000	0.08	0.04	600
19	4.00	100	500,000	0.08	0.02	600
20	4.00	120	600,000	0.08	0.02	600
21	4.00	150	750,000	0.08	0.02	600

Table 3.7. Summary of the experimental conditions used for determining the apparent activation energy over 10 wt% Co-2 wt% Ce/ZrO_2 catalyst.

Experiment No	CH_4/CO_2	Total Flow (ml/min)	Partial Pressures (atm)		Temperature (°C)
			CH_4	CO_2	
22	1	100	0.08	0.08	580
23	1	100	0.08	0.08	600
24	1	100	0.08	0.08	620

Table 3.8. Summary of the experimental conditions used for determining the effect of CO partial pressure over 10 wt% Co-2 wt% Ce/ZrO_2 catalyst.

Experiment No	CH_4/CO_2	Total Flow (ml/min)	Partial Pressures (atm)				Temperature (°C)
			CH_4	CO_2	CO	H_2	
25	1	100	0.08	0.08	0.015	-	600
26	1	100	0.08	0.08	0.030	-	600
27	1	100	0.08	0.08	0.045	-	600
28	1	100	0.08	0.08	0.060	-	600

Table 3.9. Summary of the experimental conditions used for determining the effect of H_2 partial pressure over 10 wt% Co-2 wt% Ce/ZrO_2 catalyst.

Experiment No	CH_4/CO_2	Total Flow (ml/min)	Partial Pressures (atm)				Temperature (°C)
			CH_4	CO_2	CO	H_2	
29	1	100	0.08	0.08	-	0.015	600
30	1	100	0.08	0.08	-	0.030	600
31	1	100	0.08	0.08	-	0.045	600
32	1	100	0.08	0.08	-	0.060	600
33	1	100	0.08	0.08	-	0.075	600

4. RESULTS AND DISCUSSIONS

The results and discussion part of this thesis consists of two parts:

- Performance analysis of CDRM over 5 wt% Co-2 wt% Ce/δ-Al_2O_3 catalyst,
- Kinetic experiments over 10 wt% Co-2 wt% Ce/ZrO_2 catalysts

4.1. Performance analysis of CDRM over 5 wt% Co-2 wt% Ce/δ-Al_2O_3 catalyst

The aim of this part of the work was to analyse the performance of 5 wt% Co-2 wt% Ce/ZrO_2 catalyst. Ce was used as a promoter and was added by sequential impregnation method. The purpose of Ce addition was to regulate surface oxygen transfer, which plays a direct role in carbon removal. In the CDRM performance tests, the effects of CH_4/CO_2 feed ratio, space velocity and reaction temperature on the activity, selectivity and stability of the catalyst were studied.

4.1.1. Catalyst Characterization Tests

In general, the activity of the catalysts is strongly related with the dispersion and structure of the active metal(s) on the support surface. On the other hand, the amount and type of deposited carbon directly affects the stable performance of the CDRM catalysts.

The XRD pattern of freshly reduced 5 wt% Co-2wt% Ce/δ-Al_2O_3 catalyst, given in Figure 4.1, revealed that alumina support existed in both alumina and aluminum oxide phases. No peak corresponding to metallic phases was detected indicating high dispersion of cobalt and ceria on δ-Al_2O_3 support.

The microstructural properties and metal dispersion of the freshly reduced 5 wt% Co-2 wt% Ce/δ-Al_2O_3 as well as carbon deposition on the spent catalyst were characterized by using SEM and SEM-EDX. The bright area images of freshly reduced and spent 5 wt% Co-2 wt% Ce/δ-Al_2O_3 samples are given in Figures 4.2(a) and 4.2(b), respectively. SEM images show that the metals are dispersed well except the relatively high population areas

with similar metal particle size (Figure 4.2(a)) but carbon deposition covers a significant portion of the catalyst surface (Figure 4.2(b)).

The metal mappings of the Co, Ce and Al on freshly reduced (Figures 4.3(a,c,e), respectively) and on spent catalyst samples (Figures 4.3(b,d,f), respectively) confirms the well dispersion of Co and Ce with a good homogeneity on freshly reduced samples (Figures 4.3(a,c)) but there was a carbon deposition during the reaction severe enough to cover not only the significant portion of Co centers but also the Ce centers (Figures 4.3(b,d)). The results show that carbon deposition blocks the methane dehydrogenation sites and, as it covers the Ce sites, also halts the surface oxygen transfer and carbon gasification mechanism. Additionaly, the weight percentages of the metallic species on the surface of the freshly reduced and spent samples were obtained from EDS analysis of the area given in SEM microgram are tabulated in Table 4.1. Results show that half of the Co sites and one third of Ce sites were covered with carbon. Considering the fact that methane dehyrogenation is mostly catalyzed by Co sites, coke deposition and consequent blockage is more severe on those sites.

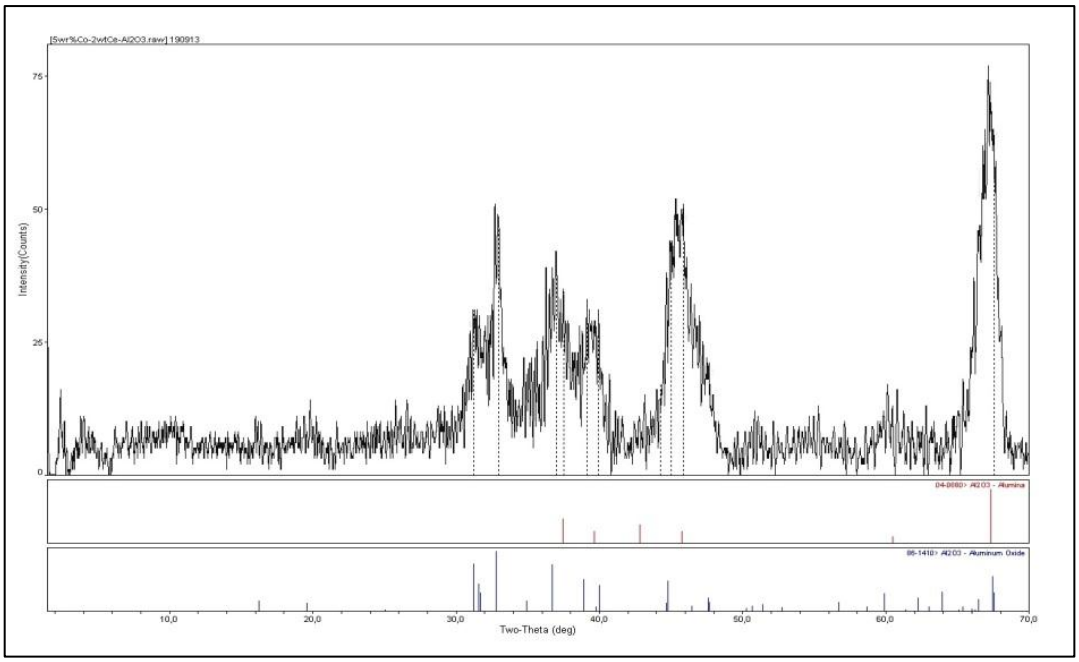

Figure 4.1. XRD analysis of freshly reduced 5 wt% Co-2 wt% Ce/δ-Al_2O_3 catalyst.

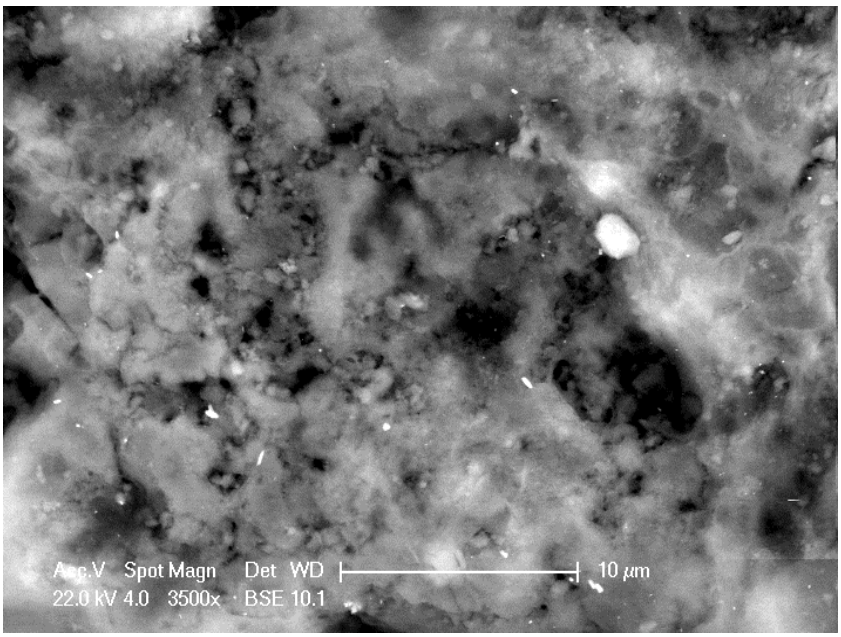

(a)

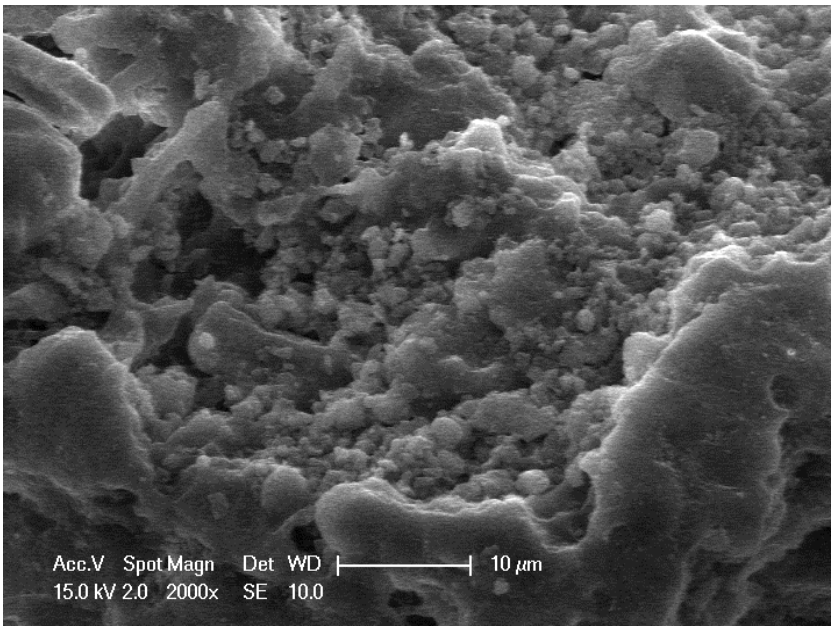

(b)

Figure 4.2. SEM bright area image of freshly reduced and spent 5 wt% Co-2 wt% Ce/δ-Al_2O_3 catalyst for CH_4/CO_2 feed ratio of 1/2 T=800°C (a) SEM bright area image of freshly reduced catalyst (b) SEM bright area image of the spent catalyst.

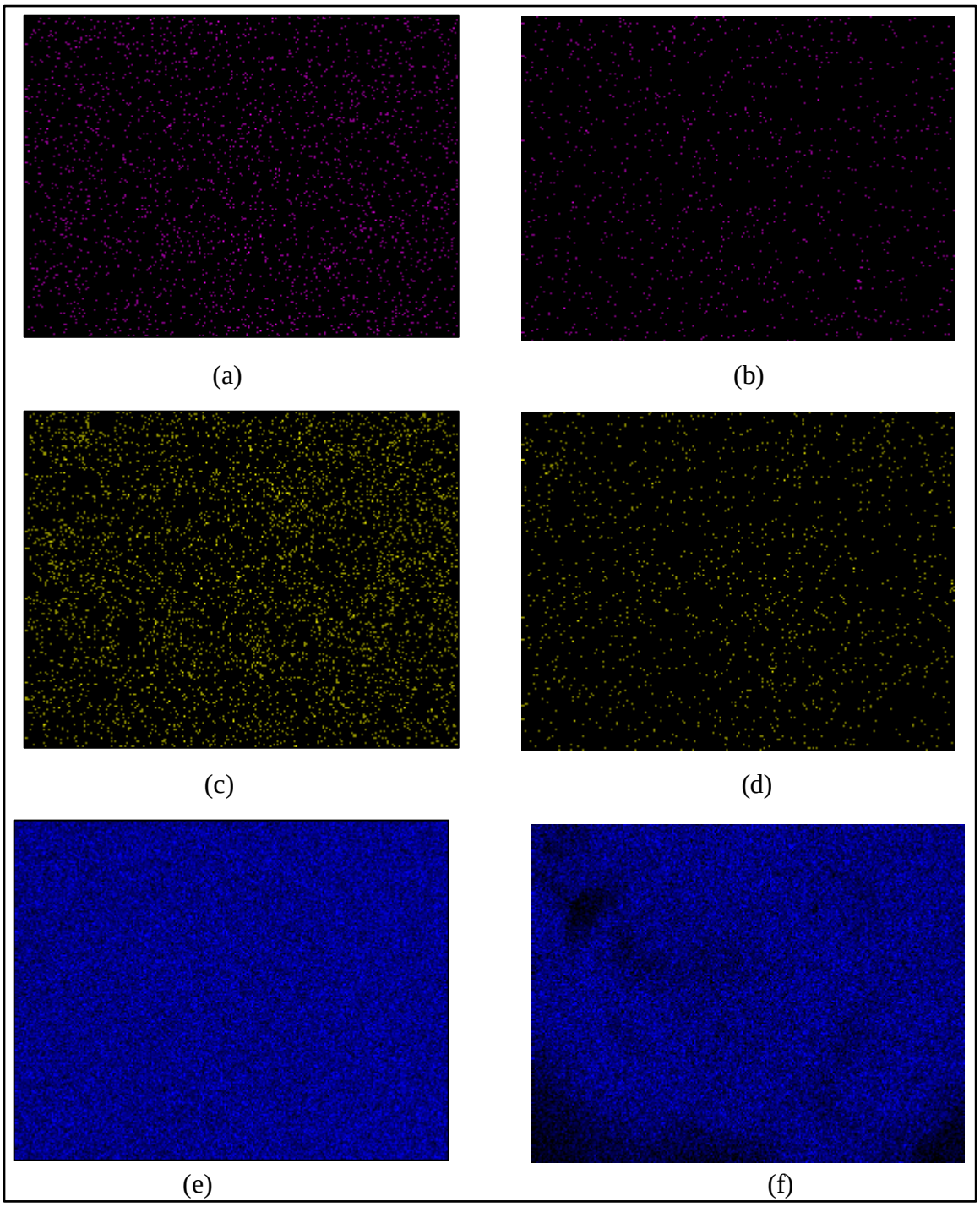

Figure 4.3. Co-Ce-Al mapping of freshly reduced and spent 5 wt% Co-2 wt% Ce/δ-Al_2O_3 catalyst samples (a) Co on fresh catalyst (b) Co after coke formation (c) Ce on fresh catalyst (d) Ce after coke formation (e) Al on fresh catalyst (f) Al after coke formation.

Table 4.1. Weight percentages of the surface metallic species from SEM-EDX data (5 wt% Co-2 wt% Ce/δ-Al_2O_3).

Catalyst	Co wt%	Ce wt%	C wt%
Co-Ce/ δ-Al_2O_3 (fresh)	4.84	2.41	1.07
Co-Ce/ δ-Al_2O_3 (used)	2.38	1.63	3.18

4.1.2. Performance Tests

The activity, stability and selectivity characteristics of the catalysts were investigated for different reaction conditions given in Section 3. The CH_4 and CO_2 conversions and H_2/CO ratio in the product stream were calculated by using the formulas below:

$$Conversion\ (\%) = \frac{[C]_{in} - [C]_{out}}{[C]_{in}} \times 100 \tag{4.1}$$

$$\frac{H_2}{CO} = \frac{[C]_{H_2}}{[C]_{CO}} \tag{4.2}$$

where C is the percentage by volume.

CH_4 and CO_2 conversion values were used as measures of activity while H_2/CO ratio in the product stream showed the selectivity. In terms of selectivity, the aim was getting closer to 1 which is the reactant rato of syngas in Fischer-Tropsch reaction.

4.1.2.1. The Effect of Temperature. The effect of temperature on CH_4 and CO_2 conversions and H_2/CO ratio is given in Figures 4.4- 4.6 for the reactions at 20000 mL/h g-catalyst space velocity with CH_4/CO_2 ratio of 1/1. While the reaction did not occur at 650°C, initial CH_4 conversions of 700°C and 800°C were 64% and 69%, respectively. At 700°C, catalyst showed a more stable performance than at 800°C although its initial conversion was lower. The same profile was observed for CO_2 conversion with initial values of 73% and 79% at 700°C and 800°C, respectively. The catalyst loses its activity

completely in 90 min. time-on-stream at 800°C. On the other hand, CH_4 conversion decreases rather gradually in the tests conducted at 700°C; the complete activity loss is observed at 210 min. time-on-stream. H_2/CO ratio changed between 0.5 and 0.8.

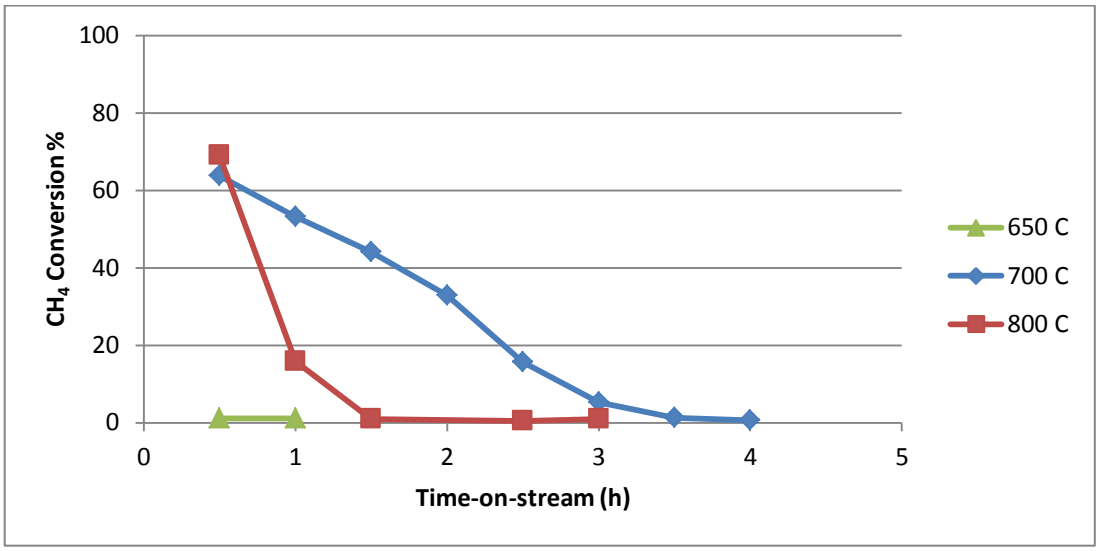

Figure 4.4. CH_4 conversion with respect to time-on-stream for CH_4/CO_2 feed ratio of 1/1.

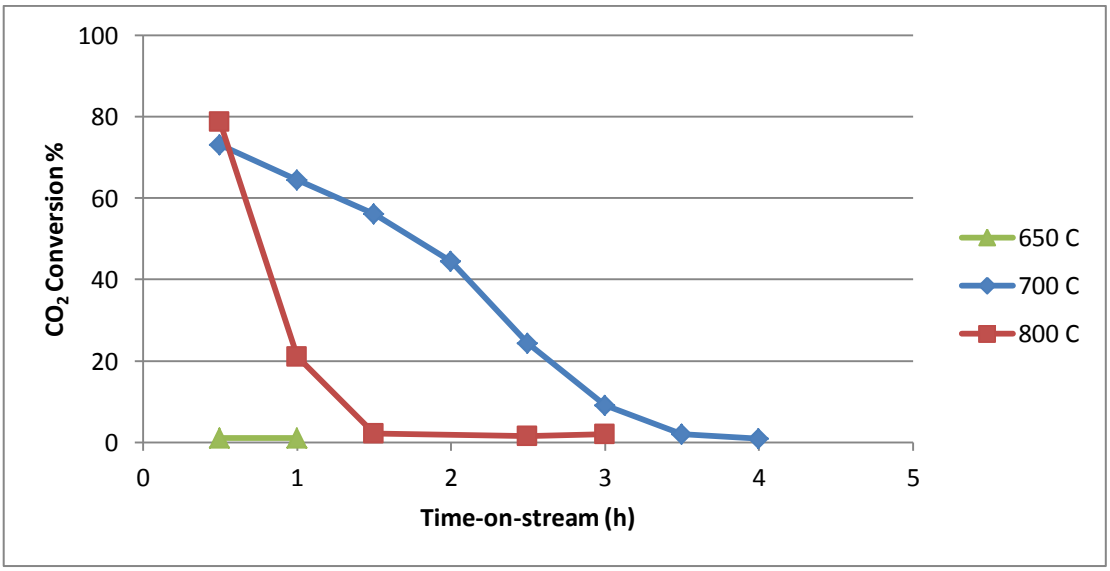

Figure 4.5. CO_2 conversion with respect to time-on-stream for CH_4/CO_2 feed ratio of 1/1.

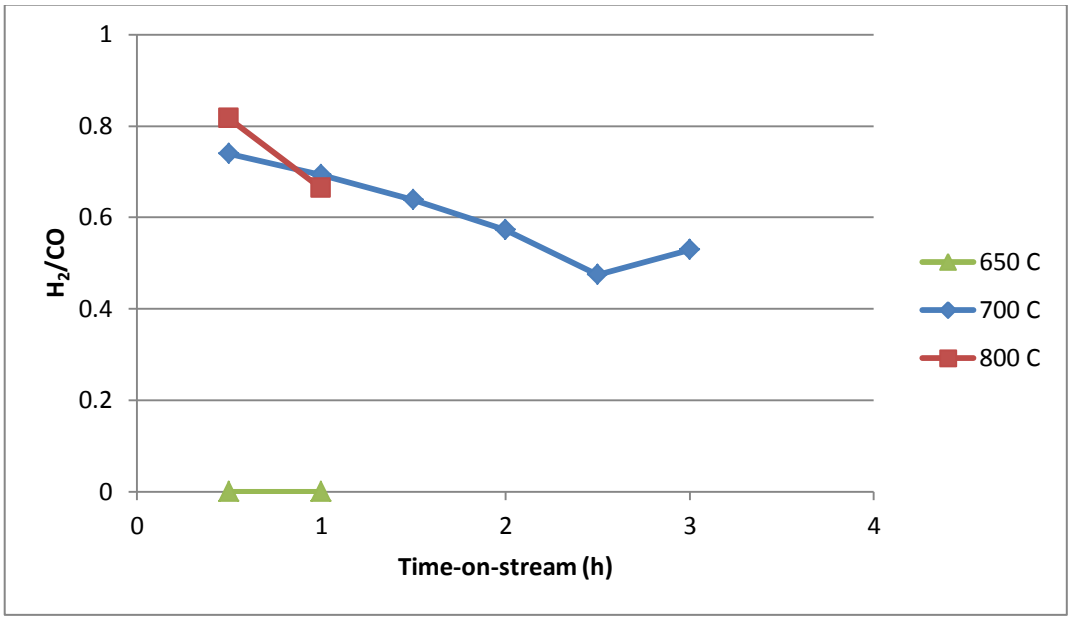

Figure 4.6. H_2/CO ratio with respect to time-on-stream for CH_4/CO_2 feed ratio of 1/1.

Figures 4.7-4.9 show the conversion values and stability results for the experiments conducted with CH_4/CO_2 ratio of 1/2. Initial CH_4 conversions of 650°C, 700°C and 800°C were 59%, 69% and 80%, respectively. At 650°C and 700°C, catalyst showed a more stable performance than at 800 °C although its initial conversions were lower. The same profile was observed for CO_2 conversion, with initial values of 52%, 58% and 69%, respectively. H_2/CO ratio changed between 0.5 and 0.9.

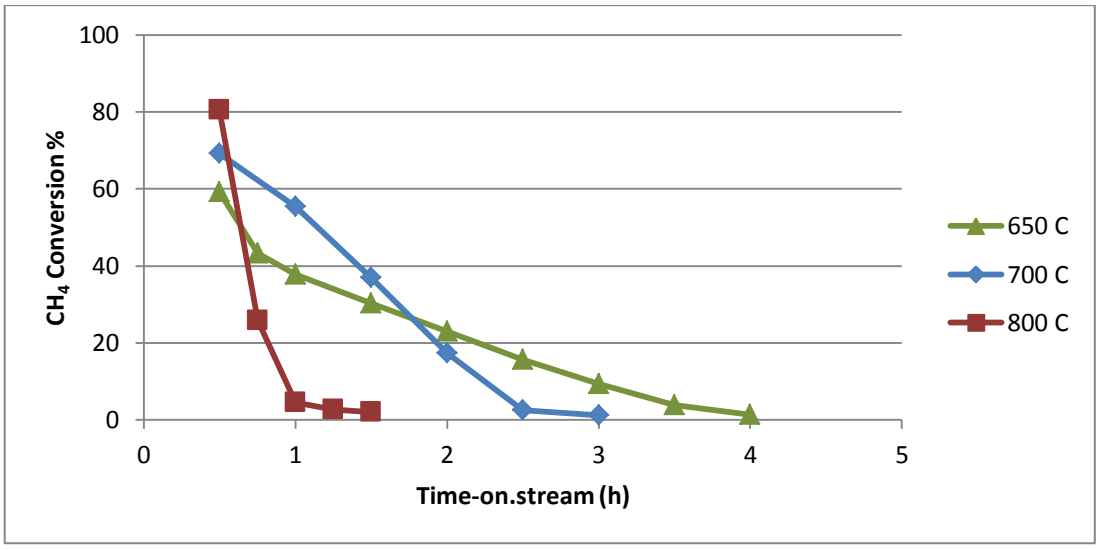

Figure 4.7. CH_4 conversion with respect to time-on-stream for CH_4/CO_2 feed ratio of 1/2.

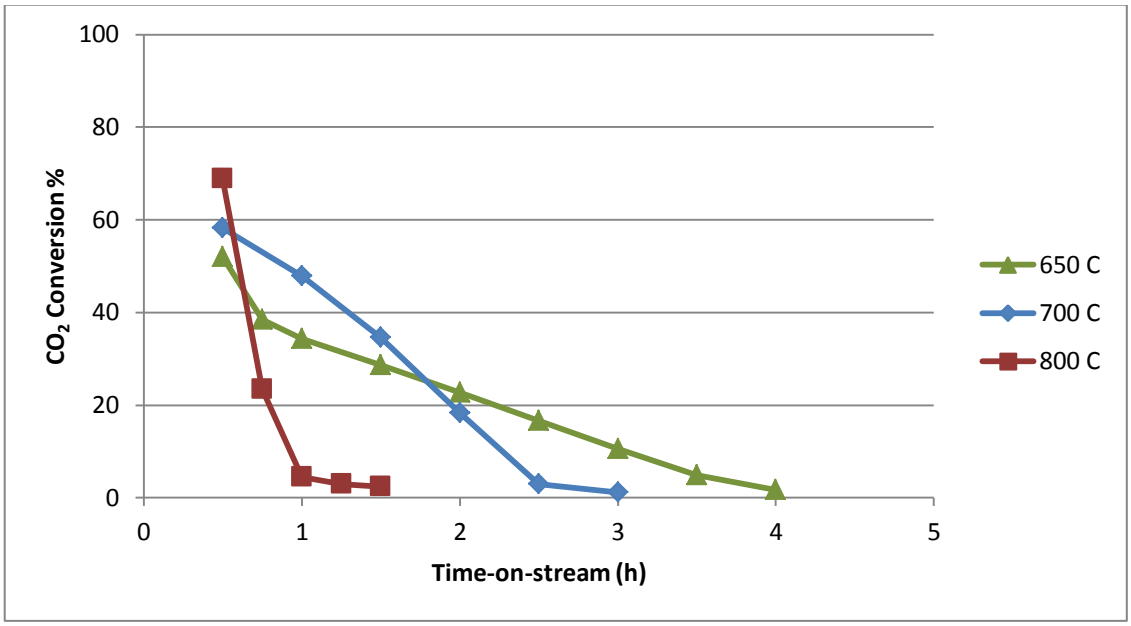

Figure 4.8. CO_2 conversion with respect to time-on-stream for CH_4/CO_2 feed ratio of 1/2.

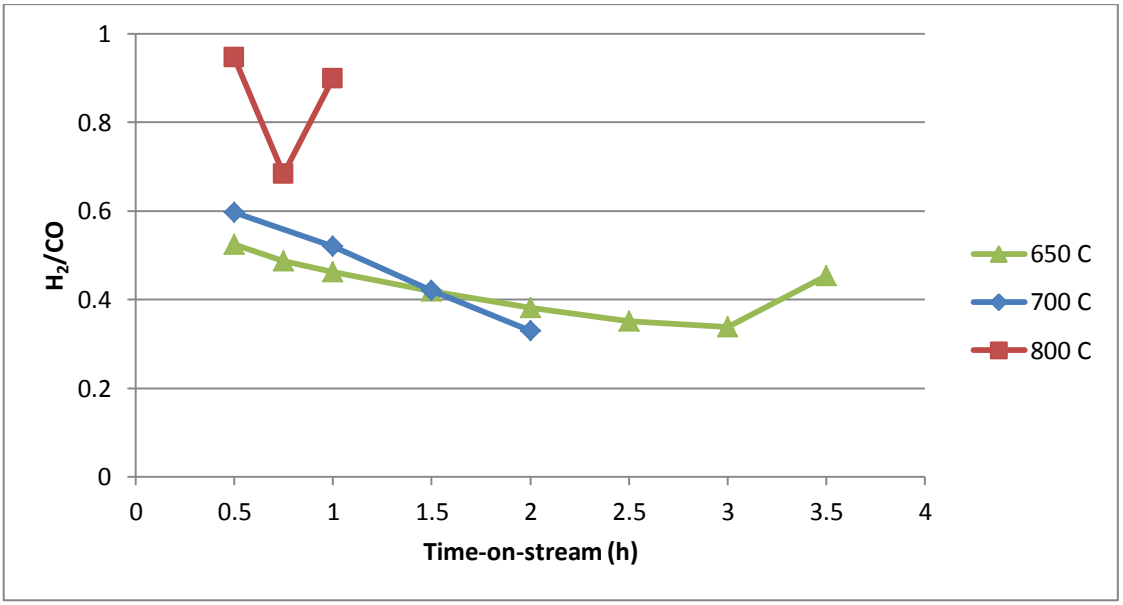

Figure 4.9. H_2/CO product ratio with respect to time-on-stream for CH_4/CO_2 feed ratio of 1/2.

Although it was clearly observed that increasing the temperature increased the activity, catalyst deactivation is relatively slower at low temperatures. Moreover, comparision between CH_4/CO_2 feed ratios revealed that the ratio of 1/2 yielded higher methane conversion and lower carbon dioxide conversion than those observed for the feed ratio of 1/1.

4.1.2.2. The Effect of Space Velocity. The effect of space velocity on the CDRM performance was observed on the basis of the activity results obtained for three different space velocities, 10000 mL/h g-catalyst, 20000 mL/h g-catalyst, 30000 mL/h g-catalyst with CH_4/CO_2=1 feed ratio at 700°C (Figures 4.10-4.12). For space velocity of 30000 mL/h g-catalyst no CDRM activity was observed. On the otherhand, for the space velocities of 10000 mL/h g-catalyst and 20000 mL/h g-catalyst, almost the same performance was observed with initial CH_4 conversion value of 64% and 63%, respectively. Initial CO_2 conversion was found 73% for each case and H_2/CO conversion remained between 0.4 and 0.75. For both space velocity values, the catalyst lost its CDRM activity within 210 min. time-on-stream.

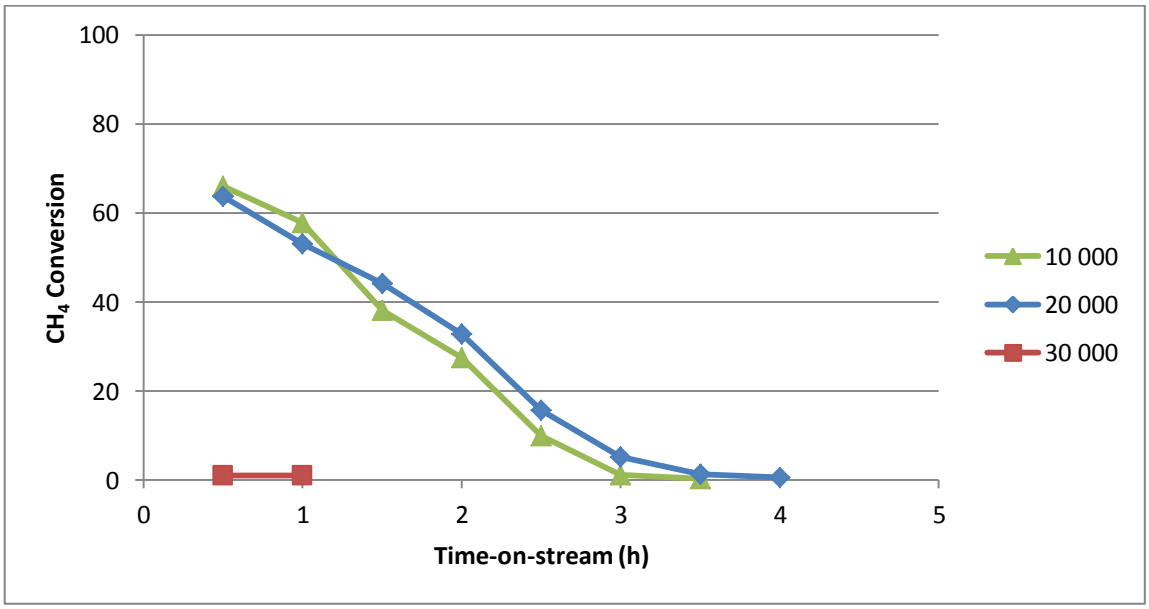

Figure 4.10. CH_4 conversion with respect to time-on-stream for CH_4/CO_2 feed ratio of 1/1 T= 700°C.

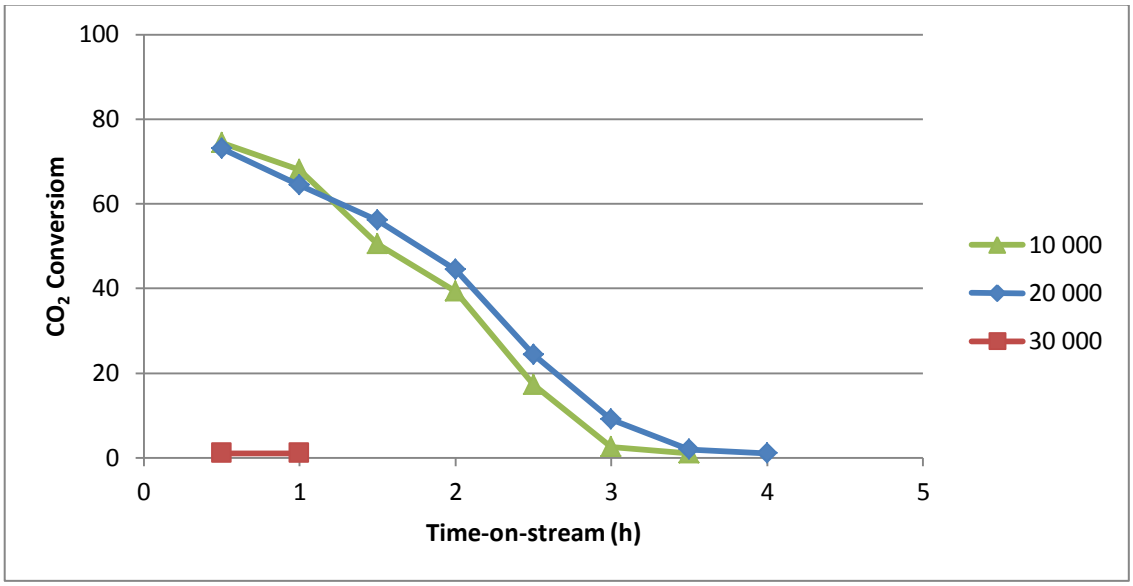

Figure 4.11. CO_2 conversion with respect to time-on-stream for CH_4/CO_2 feed ratio of 1/1 T=700°C.

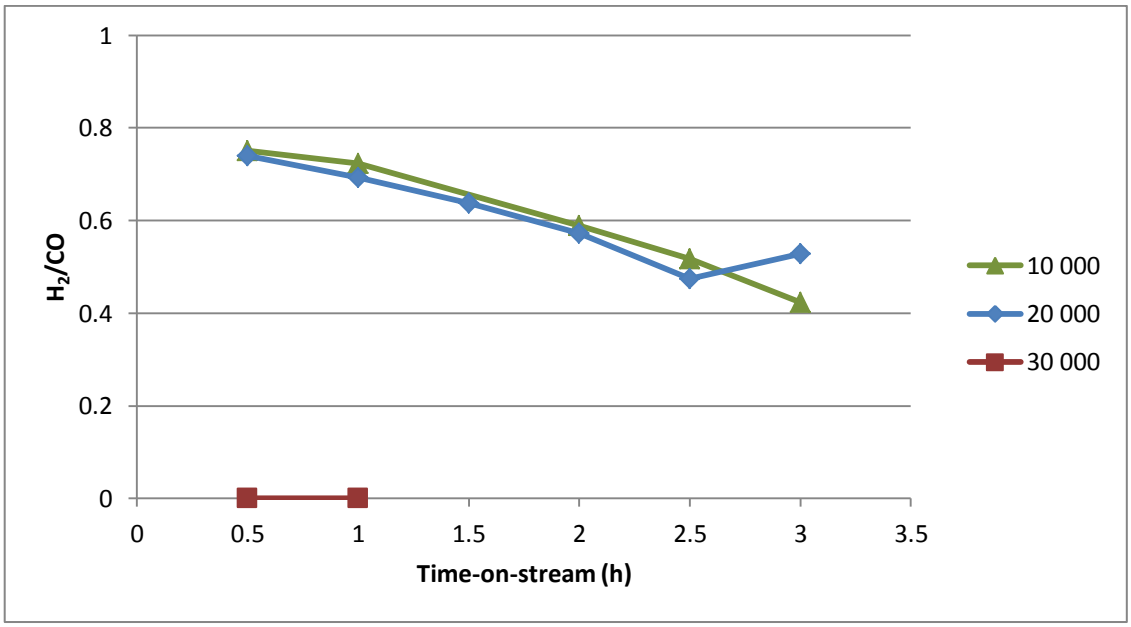

Figure 4.12. H_2/CO product ratio with respect to time-on-stream for CH_4/CO_2 feed ratio of 1/1 T=700°C.

4.2. Kinetic Experiments over 10 wt% Co-2 wt% Ce/ZrO_2 Catalyst

The aim of the kinetic study over 10 wt% Co-2 wt% Ce/ZrO_2 catalyst was to obtain a rate expression and derive a kinetic model for CDRM over the catalyst under fully realistic reaction conditions.

CDRM is not a stoichiometry-independent reaction; the reaction network includes the reaction steps described below (Nandini *et al.*, 2006).

$$CH_4 + CO_2 \leftrightarrow 2CO + 2H_2 \quad (Carbon\ Dioxide\ Reforming\ of\ Methane) \qquad (4.3)$$

$$H_2 + CO_2 \leftrightarrow CO + H_2O \quad (Reverse\ water-gas\ shift) \qquad (4.4)$$

$$CO_2 + 4H_2 \leftrightarrow CH_4 + 2H_2O \quad (CO_2\ methanation) \qquad (4.5)$$

$$CO + 3H_2 \leftrightarrow CH_4 + H_2O \quad (CO\ methanation) \qquad (4.6)$$

$$CH_4 + H_2O \leftrightarrow CO + 3H_2 \quad (Steam\ Reforming) \qquad (4.7)$$

$$2CO \leftrightarrow C + CO_2 \quad (Boudouard\ reaction) \qquad (4.8)$$

$$CH_4 \leftrightarrow C + 2H_2 \quad (Methane\ decomposition) \qquad (4.9)$$

$$C + H_2O \leftrightarrow CO + H_2 \quad (Coke\ gasification) \qquad (4.10)$$

The temperature of the kinetic study was choosen as 600°C to be sure that the side reactions do not get involved with the dry reforming and it was kept constant if not specified otherwise. The experiments were performed under diffrential conditions at atmospheric pressure using 12 mg catalyst. The total feed flow rate was changed between 100-150 mL/min in order to obtain significantly lower conversion levels within the range up to 25 percent, which were far away from the corresponding thermodynamic equilibrium under the reaction conditions, guaranteeing where CDRM reaction was controlled only by kinetics.

The catalyst mass-based reaction rates for the kinetic measurements can be calculated from Equation 4.9 .

$$-r_{CH_4} = \frac{x_{CH_4} F_{CH_4}}{w_{cat}} \tag{4.11}$$

where x_{CH_4} is CH_4 conversion, F_{CH_4} is CH_4 flow rate in the feed in mL/min converted to mmol/s, w_{cat} is the catalyst weight in g and $-r_{CH_4}$ is the reaction rate in mmol/g s.

The kinetic tests consist of a series of experiments which were performed at different initial reactant concentrations with the varying w_{cat} /F_{CH_4} ratio. The initial rates were calculated by differentiating the data and extrapolating it to zero times.

4.2.1. Catalyst Characterization Tests

Freshly reduced 10 wt% Co-2 wt% Ce/ZrO_2 catalyst were tested using SEM to obtain information on metal dipersion properties. Secondary electron and X-ray analytical mapping images given in Figure 4.13 and 4.14 reveal that the metals are well dispersed on the catalyst. Additionaly, the weight percentages of the metallic species on fresh and used catalysts are tabulated in Table 4.2. The metal weight percentages are obtained as 8.89 wt% for Co and 5.00 wt% for Ce from EDS analysis (Table 4.2).

The XRD pattern of freshly reduced 10 wt% Co-2 wt% Ce/ZrO_2 catalyst sample given in Figure 4.15 confirms the SEM and EDS result; no Co or Ce metallic phase was detected implying well dispersion of metals.

Table 4.2. Weight percentages of the surface metallic species from SEM-EDX data (Freshly reduced Co-Ce/ZrO_2 catalyst).

Catalyst	Co wt%	Ce wt%
Co-Ce/ ZrO_2	8.89	5.00

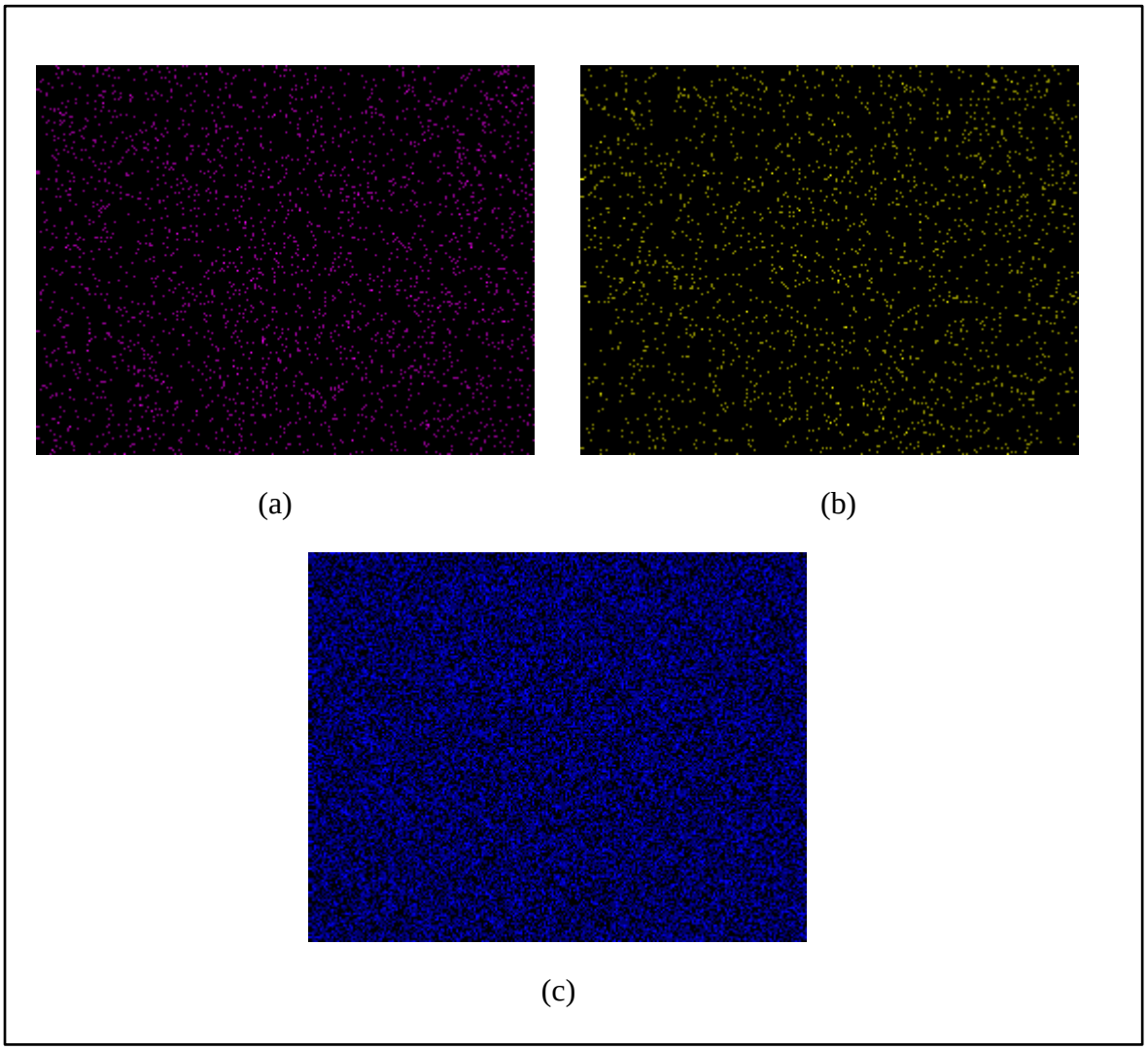

Figure 4.13. Co-Ce-Zr mapping of freshly reduced 10 wt% Co-2 wt% Ce/ZrO_2 catalyst samples (a) Co mapping of freshly reduced catalyst (b) Ce mapping of freshly reduced catalyst (c) Zr mapping of freshly reduced catalyst.

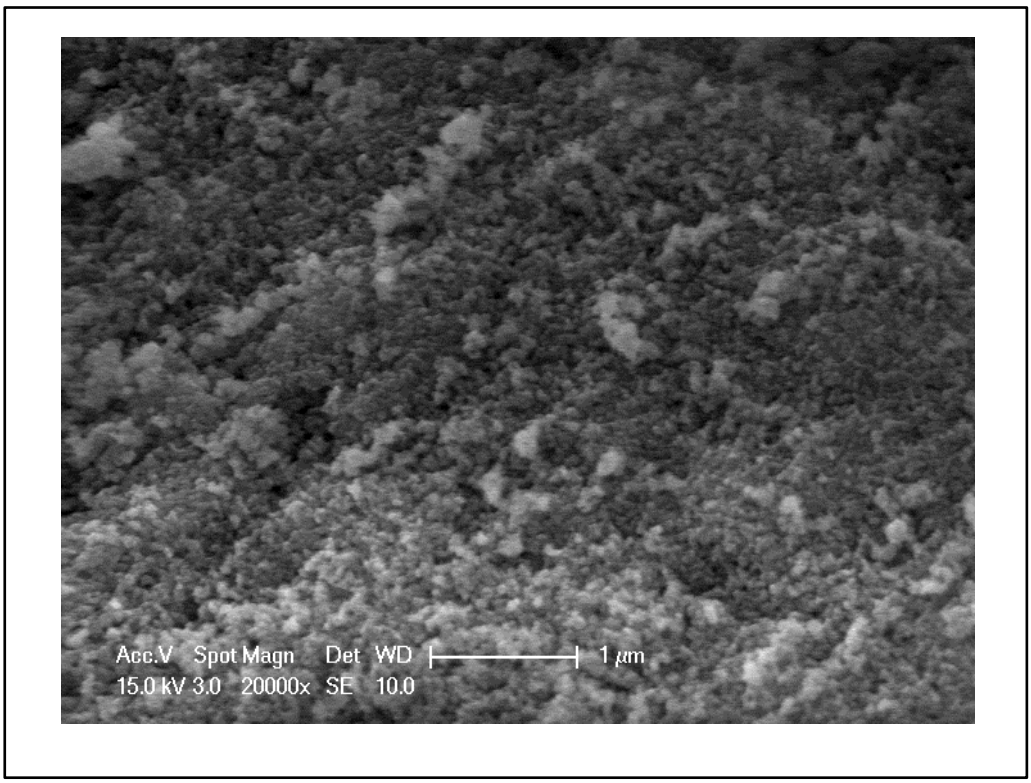

Figure 4.14. SEM bright area image of freshly reduced 10 wt% Co-2 wt% Ce/ZrO_2 catalyst.

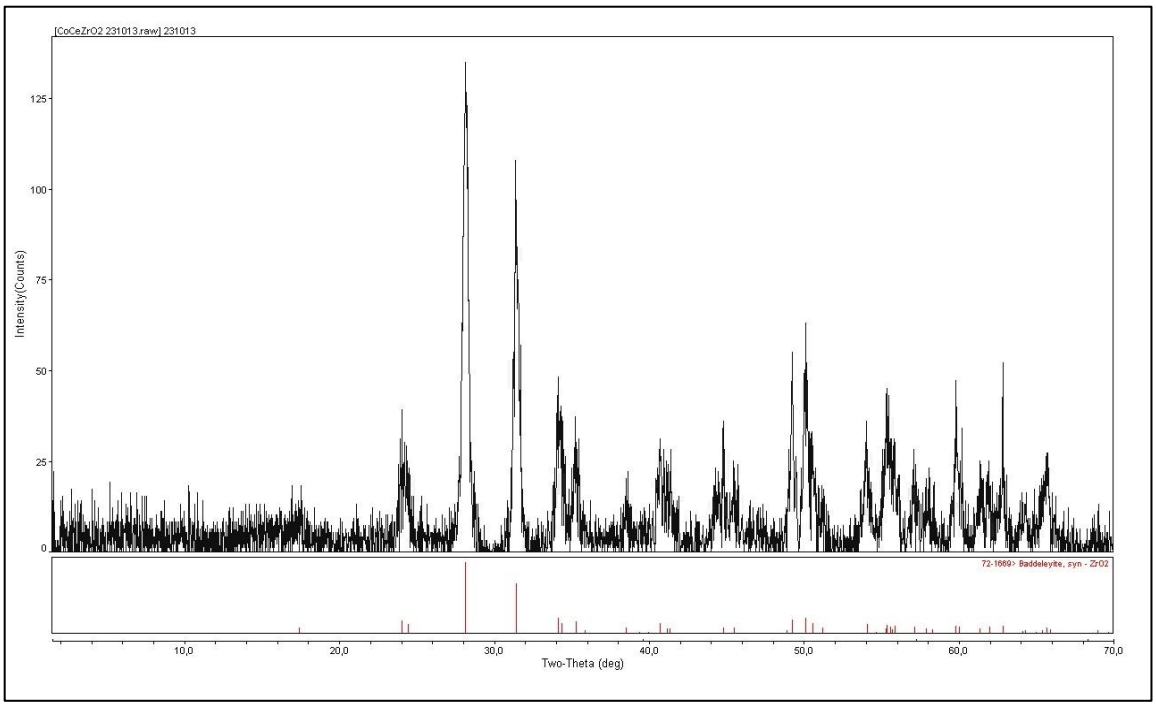

Figure 4.15. XRD analysis of freshly reduced 10 wt% Co-2 wt% Ce/ZrO_2 catalyst.

4.2.2. Apparent Activation Energies

The apparent activation energies were calculated based on the consumption rates of CH_4 and CO_2, by repeating the experiment no 10 given in Table 3.6 at 580°C and 620°C (Table 3.7). The experimental data were taken after 90 min time-on-stream. The linear Arrhenius plot of ln(-r) versus (1/T) is given in Figure 4.16 and 4.17.

The slope of the straight lines in the Arrhenius plot gives ($-E_A/R$), from which the activation energy of the reaction (E_A) is calculated as 61.3 kJ mol^{-1} for CH_4 and 50.53 kJ mol^{-1} for CO_2. It is worth noting that the activation barrier for CH_4 is higher than that for CO_2 consumption, which is in agreement with reported values in the literature given in Table 2.1.

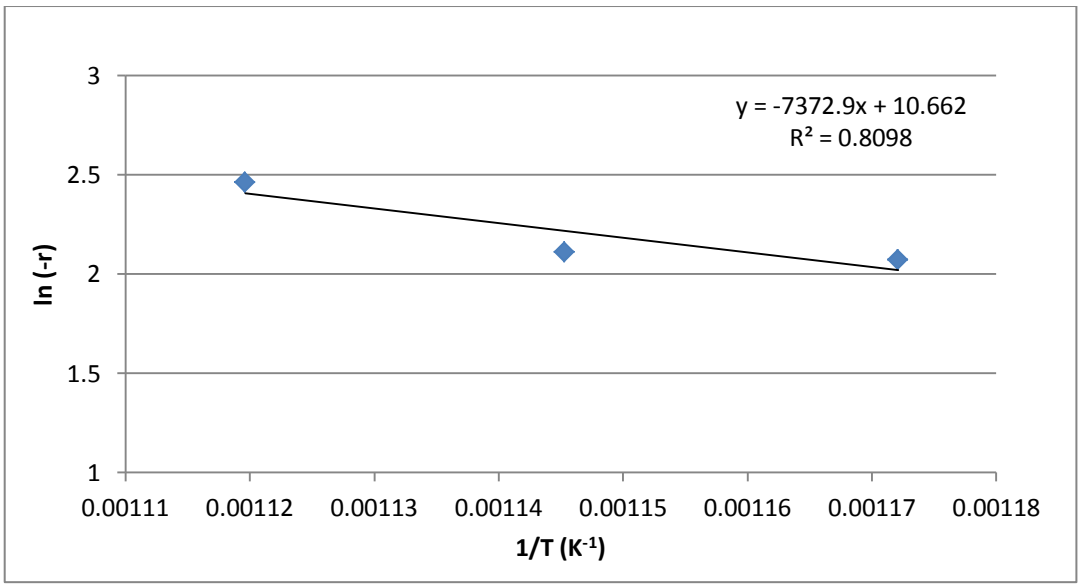

Figure 4.16. Arrhenius plot for CH_4.

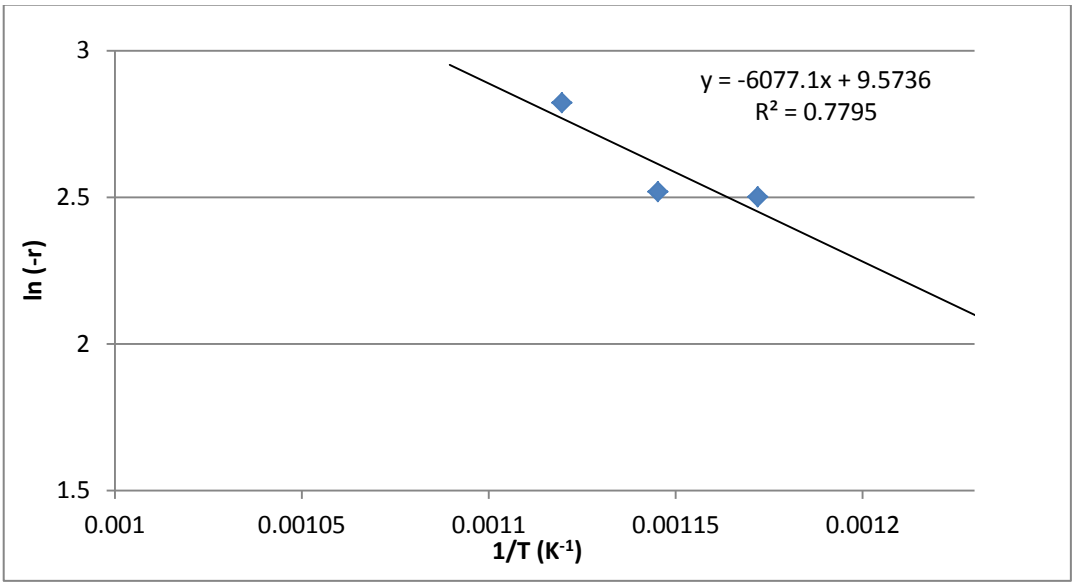

Figure 4.17. Arrhenius plot for CO_2.

4.2.3. Power-Law Type CDRM Kinetics

The partial pressure dependencies were determined at 600°C by keeping a constant partial pressure of 0.08 atm of one reactant while the other one was changed between 0.02 atm and 0.08 atm. Total flow rate of the feed was manipulated between 100-150 mL/min to obtain significantly lower conversions within the range values 5-25 percent, which were far away from the corresponding thermodynamic equilibrium. Nitrogen was used as inert to keep total flow constant and to maintain the pressure close to atmospheric. Experiments performed in this study are presented at Tables 3.6-3.9 in detail.

The power-law type rate equation for CDRM is given in equation 4.12. Evaluation of the rate parameters requires calculation of initial reaction rates. The reaction rates which were given in Table 4.3 were calculated from slopes of the conversion versus residence time plots given in Appendix A. Variation of the reaction rate as a function of methane partial pressure graphs are given in Figures 4.18 and 4.19.

$$(-r_{CH_4}) = k\left(P_{CH_4}\right)^{\alpha}\left(P_{CO_2}\right)^{\beta} \tag{4.12}$$

Table 4.3. Initial reaction rates calculated from conversion-residence time data.

Experiment No.	P_{CH4}	P_{CO2}	W_{cat}/ F_{CH4} (g.s.mmol^{-1})	Conversion %		Initial Reaction Rate (mmol g^{-1} s^{-1})
				CH_4	CO_2	
1	0.02	0.08	8.064	14.86	11.02	0.018548
2			6.72	12.58	7.31	
3			5.376	-	-	
4	0.04	0.08	4.032	14.91	17.07	0.040184
5			3.36	13.67	12.83	
6			2.688	12.53	14.1	
7	0.06	0.08	2.688	14.98	19.64	0.060840
8			2.24	13.75	18.9	
9			1.68	12.27	17.02	
10	0.08	0.08	2.016	16.62	24.98	0.082442
11			1.68	14.75	19.84	
12			1.344	9.95	17.31	
13	0.08	0.06	2.016	23.99	42.56	0.10115
14			1.68	14.50	32.97	
15			1.344	11.33	23.36	
16	0.08	0.04	2.016	22.60	57.5	0.099778
17			1.68	15.55	40.3	
18			1.344	11.20	33.06	
19	0.08	0.02	2.016	20.61	82.5	0.099563
20			1.68	16.17	76.47	
21			1.344	13.27	65.8	

The resulted rate versus partial pressure data were used to estimate the reaction parameters via non-linear regression analysis with Levenberg-Marquardt algorithm provided in the computer software POLYMATH 5.1. The calculated rate parameters are given in Table 4.4. Comparision between experimental rate values and calculated rate values are presented in Appendix B. The reaction orders indicate that the reaction rate is proportional to the partial pressure of methane while there is a small inhibition effect of

carbon dioxide. This may be due to active site competition between CO_2 and CH_4 molecules, especially for the sites on which methane is activated.

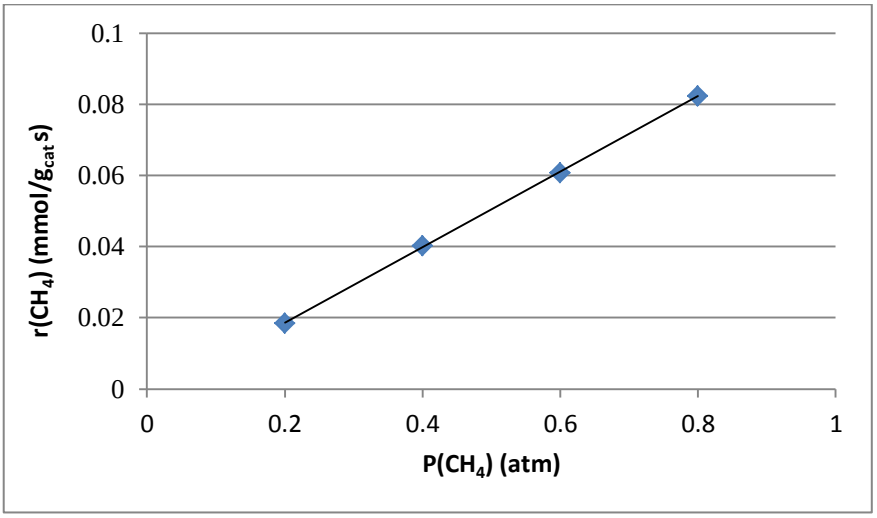

Figure 4.18. Variation of the reaction rate as a function of methane partial pressure.

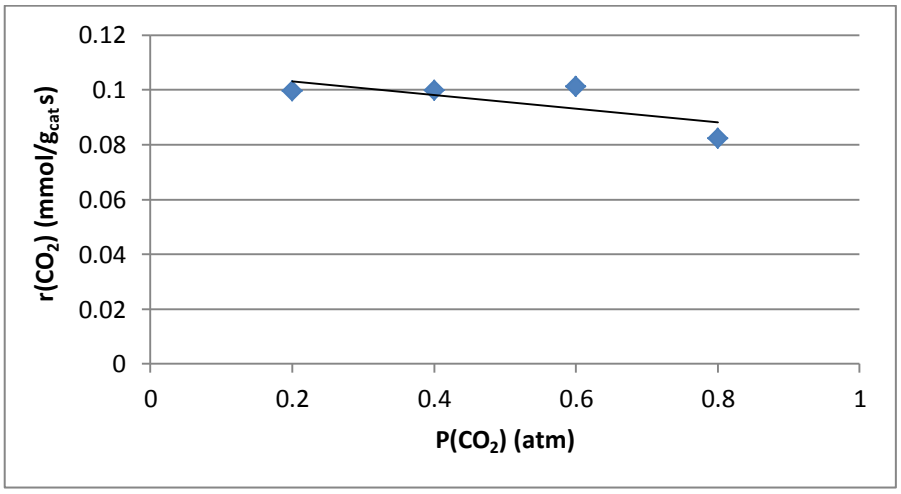

Figure 4.19. Variation of the reaction rate as a function of carbon dioxide partial pressure.

Table 4.4. Estimated reaction rate parameters.

Reaction Order		k	σ^2 (mmol.g^{-1}.s^{-1})^2
(α)	(β)		
1.1926	-0.0968	0.00921 mmol g^{-1} s^{-1} atm$^{-1.118}$	4.16×10^{-5}

4.2.4. Mixed Feed Tests: Effect of CO on CDRM Rate

Carbon monoxide with inlet partial pressure varying from 0.015-0.06 atm was added to feed stream while keeping partial pressures of CH_4 and CO_2 constant in order to find out the effect of CO on the CDRM rate. Reaction tests given in Table 3.8 were carried out with 12 mg catalyst at 600°C. Obtained conversions and reaction rates are given in Tables 4.5 and 4.6, respectively.

Table 4.5. Effect of CO partial pressure on CH_4 and CO_2 conversions.

CO %	CH_4 Conversion %	CO_2 Conversion %
0	16.62	24.98
1.5	13.51	20.85
3	17.32	24.39
4.5	19.06	25.91
6	12.03	16.23

Table 4.6. Effect of CO partial pressure on CDRM rates.

Experiment No.	Partial Pressures (atm)			Reaction Rate ($mmol\ g^{-1}\ s^{-1}$)
	CH_4	CO_2	CO	
25	0.08	0.08	0.015	0.067014
26	0.08	0.08	0.030	0.085863
27	0.08	0.08	0.045	0.094544
28	0.08	0.08	0.060	0.059623

The form of the power-law type rate expression is given in Equation 4.13. The reaction order of CO was evaluated by non-linear regression, using the data of CH_4 consumption rates in the presence of CO in the feed and corresponding partial pressure of CO. Related graph is given in Figure 4.20. The correlation coefficient (R^2) was found as 0.0007. Because it is a small value, any observation could not be posibble for the effect of CO partial pressure on CDRM rate.

$$(-r_{CH_4}) = k\left(P_{CH_4}\right)^{\alpha}\left(P_{CO_2}\right)^{\beta}(P_{CO})^{\delta} \quad (4.13)$$

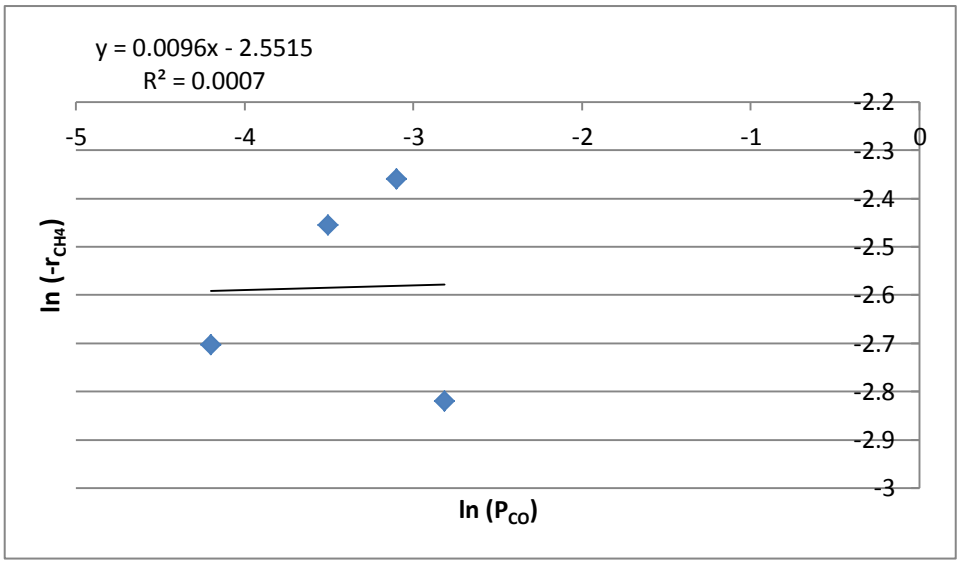

Figure 4.20. The effect of CO partial pressure on CDRM rate.

4.2.5. Mixed Feed Tests: Effect of H_2 on CDRM Rate

The presence of H_2 in the feed may affect the CDRM rate. In order to see the effect of H_2 partial pressure on the rate, H_2 with inlet partial pressures varying between 0.03-0.075 atm was added to feed stream while keeping partial pressures of CH_4 and CO_2 constant. 12 mg catalyst was used at each test and reaction temperature was kept constant at 600°C. The partial pressures of the components, obtained conversions and reaction rates are given in Tables 4.7 and 4.8. The form of the power-law type rate expression is given in Equation 4.14.

The reaction order of H_2 was evaluated by non-linear regression, using the data of CH_4 consumption rates in the presence of H_2 in the feed and corresponding partial pressure of H_2 Related graph is given in Figure 4.21. The correlation coefficient (R^2) was found as 0.199. Because it is a small value, any observation could not be posibble for the effect of H_2 partial pressure on CDRM rate. However, increase of H_2 partial pressure led to a further CO_2 consumption which can be attributed to reverse water-gas shift reaction.

Table 4.7. Effect of H_2 partial pressure on CH_4 and CO_2 conversions.

H_2 %	CH_4 Conversion %	CO_2 Conversion %
0	16.62	24.98
3	14.02	27.11
4.5	12.24	34.46
6	12.63	36.78
7.5	17.58	41.01

Table 4.8. Effect of H_2 partial pressure on CDRM rates.

Experiment No.	Partial Pressures (atm)			Reaction Rate (mmol g^{-1} s^{-1})
	CH_4	CO_2	H_2	
29	0.08	0.08	0.03	0.069544
30	0.08	0.08	0.045	0.060714
31	0.08	0.08	0.06	0.062649
32	0.08	0.08	0.075	0.087202

$$(-r_{CH_4}) = k\,(P_{CH_4})^{\alpha}\,(P_{CO_2})^{\beta}(P_{H_2})^{\gamma} \qquad (4.14)$$

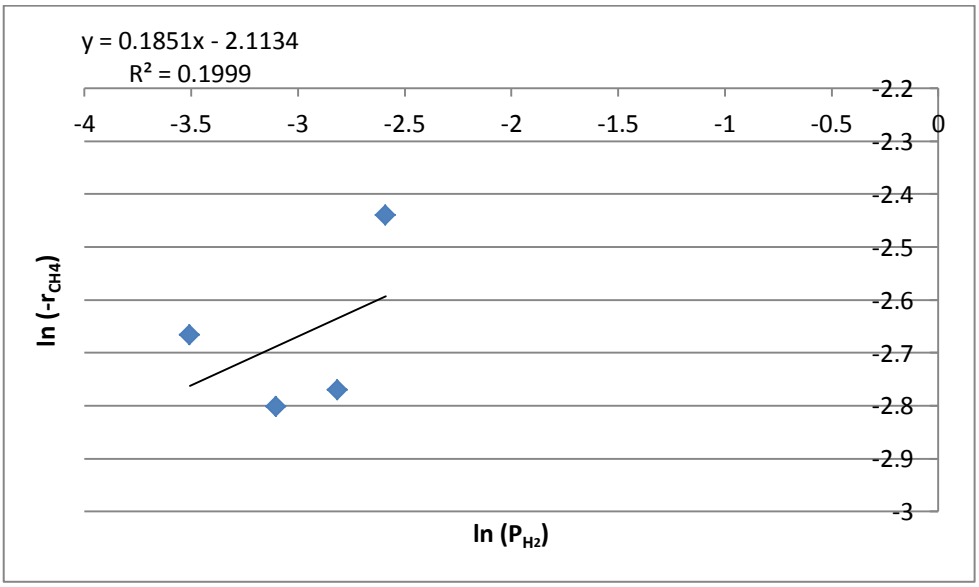

Figure 4.21. The effect of H_2 partial pressure on CDRM rate.

4.2.6. Suggested Mechanisms

A power-law type model is useful in reactor design but it is insufficient to understand the mechanistic features of CDRM. Thus, it is essential to compare experimental results obtained with proposed mechanistic CDRM rate expressions in literature.

In this work, Langmuir-Hinshelwood and Eley-Rideal type rate expressions given in Table 4.9, which were adopted from Ozkara-Aydinoglu, were used to fit the dry reforming data. Experimental CH_4 rate data were analyzed using nonlinear regression analysis with Levenberg-Marquardt algorithm provided in the computer software POLYMATH 5.1 for estimating parameters in the various kinetic models (Ozkara-Aydinoglu, 2008). The calculated model parameters are presented in Table 4.9. The equation that fits best the experimental data were determined by comparing the variance of the experimental error (σ^2) for each model and selecting the equation with the smaller variance (Ozkara-Aydinoglu, 2008). Models giving either poor correlation coefficients or negative parameter values were excluded; the calculated parameter values are given only for the models found plausible (Table 4.10). The complete set of results obtained from the non-linear regression analysis are given in the Appendix C.

In the models, the K_i values stand for the adsorption coefficients for each species. Model 1, which proposed by Mark et al.(1997) based on the Eley-Rideal type of heterogeneous model assumes that CO_2 is adsorbed on the catalyst surface in adsorption equilibrium. The slow and the rate-determining step is the reaction of adsorbed CO_2 with CH_4 from the gas phase leading directly to products.

The rate determining step was determined as the CO formation step for Model 2, proposed by Wang *et al.* (1999) for Ni/Al_2O_3 catalyst (Ozkara-Aydinoglu, 2008). On the basis of their investigation, the mechanism was simplified as:

$$CH_4 + * \rightarrow {CH_4}^* \tag{4.15}$$

$$CO_2 + * \rightarrow {CO_2}^* \tag{4.16}$$

$$CH_4{}^* \rightarrow CH_3{}^* + H \quad (4.17)$$

$$CH_3{}^* \rightarrow CH_2{}^* + H \quad (4.18)$$

$$CH_2{}^* \rightarrow CH^* + H \quad (4.19)$$

$$CH^* \rightarrow C^* + H \quad (4.20)$$

$$C^* + CO_2{}^* \rightarrow 2CO + 2^* \quad (4.21)$$

$$CO \rightarrow C + O \quad (4.22)$$

$$2H + O \rightarrow H_2O \quad (4.23)$$

$$H + H \rightarrow H_2 \quad (4.24)$$

where the CO formation step (Equation 4.21) is the rate-determining step (Ozkara-Aydinoglu, 2008).

Model 3 was proposed by Zhang and Verykios (1994) derived from a Langmuir-type model, assuming methane dissociation is the rate-determining step (Ozkara-Aydinoglu, 2008).

Model 4, proposed by Mark *et al.* (1997) and by Richardson and Paripatyadar (1990), was derived from LH model type rate expression which assumes that both reactants are adsorbed and the rate determining step is the surface reaction of the adsorbed reactants to form products H_2 and CO (Ozkara-Aydinoglu, 2008).

Model 5 was reported by Olsbye *et al.* (1997) for the kinetic studies of CDRM over Ni/La/Al_2O_3 catalyst. The observed kinetic data were found to be in fairly good agreement with the predicted L-H type rate expression. The model was validated with a laboratory scale fluidized-bed reactor. However, Olsbye *et al.* did not present the reaction mechanism from which the model was proposed (Ozkara-Aydinoglu, 2008).

Model 6 was derived from Model 1 simply by adding the inhibiting effect of CO in the denominator (Ozkara-Aydinoglu, 2008).

Model 7, reported by Olsbye et al. (1997) and Mark et al. (1997), assumes an Eley-Rideal (ER) type of heterogeneous model in which the reaction between CH_x and CO_2 is rate-limiting at low pressures of carbon dioxide. CH_4 is adsorbed on the catalyst surface and dissociates to CH_x and H. The slow and the rate determining step is the reaction of adsorbed CH_x with CH_4 from the gas phase (Ozkara-Aydinoglu, 2008).

The inhibiting effect of both CO and CH_4 is considered in Model 8.

The analysis of the kinetics data obtained over the Co-Ce/ZrO_2 system revealed that Models 1, 3, 4 and 7 fit the data with fairly low error values. Based on the analysis, (i) ER mechanisms which either has the reaction of adsorbed CO_2 with CH_4 from the gas phase leading directly to products (Model 1) or reaction between CH_x, which formed on the surface from adsorbed methane, and gas phase CO_2 (Model 7) are the rate-limiting steps; and (ii) LH mechanisms either having methane dissociation (Model 3), or surface reaction of the adsorbed reactants to form products H_2 and CO (Model 4) as the rate determining steps are found plausible. The correlations between observed rates and calculated reaction rates with the plausible mechanistic models are presented in Appendix D. The comparative analysis of the error values and the the fact that rate is highly depends on methane partial pressure but CO_2 has very little inhibitory affect, Model 1 and Model 4 seems more probable. On the other hand, the results clearly indicate that further FTIR-DRIFT analysis is necessary for finding the mechanism of CDRM reaction on Co-Ce/ZrO_2 system.

Table 4.9. Suggested rate expressions.

Model No	Proposed Rate Equations
1	$(-r_{CH_4}) = \frac{kK_{CO_2}P_{CH_4}P_{CO_2}}{(1+K_{CO_2}P_{CO_2})^2}$
2	$r_{CH_4} = \frac{k_1 P_{CH_4} P_{CO_2}}{(1+K_1 P_{CH_4})(1+K_2 P_{CO_2})}$
3	$r = \frac{aP_{CH_4}P_{CO_2}^2}{(P_{CO_2}+bP_{CO_2}^2+bP_{CH_4})^2}$
4	$(-r_{CH_4}) = \frac{kK_{CO_2}K_{CH_4}P_{CH_4}P_{CO_2}}{(1+K_{CO_2}P_{CO_2}+K_{CH_4}P_{CH_4})^2}$
5	$(-r_{CH_4}) = \frac{kP_{CH_4}P_{CO_2}}{(1+K_1P_{CH_4}+K_2P_{CO})(1+K_3P_{CO_2})}$
6	$(-r_{CH_4}) = \frac{kK_{CO_2}P_{CH_4}P_{CO_2}}{(1+K_{CO_2}P_{CO_2}+K_{CO}P_{CO})}$
7	$(-r_{CH_4}) = \frac{kK_{CH_4}P_{CH_4}P_{CO_2}^m}{(1+K_{CH_4}P_{CH_4})}$
8	$(-r_{CH_4}) = \frac{kP_{CH_4}^m P_{CO_2}^n}{(1+K_{CO_2}P_{CO_2}+K_{CO}P_{CO}+K_{CH_4}P_{CH_4})}$

Table 4.10. Model parameters.

Model No	Rate Parameters	σ^2 (mmol.g^{-1}.s^{-1})^2
1	k = 5.216 mmol.g^{-1}.s^{-1}.atm^{-1} $K_{CO_2} = 32.19$ atm^{-1}	1.59×10^{-5}
3	a = 2.345 mmol.g^{-1}.s^{-1}.atm^{-3} b = 5.511 atm^{-2} c = 0.06521 atm^{-1}	2.457×10^{-5}
4	k = 64.586 mmol.g^{-1}.s^{-1} $K_{CO_2} = 32.431$ atm^{-1} $K_{CH_4} = 0.0812$ atm^{-1}	2.012×10^{-5}
7	k = 48.941 mmol.g^{-1}.s^{-1} $K_{CH_4} = 0.01641$ atm^{-1} m = -0.1223	5.521×10^{-5}

5. CONCLUSIONS AND RECOMMENDATIONS

5.1. Conclusions

The aim of this study is to design Co-based CDRM (catalytic dry reforming of methane) catalysts and to understand the CDRM reaction kinetics over their surface. Since the thesis consists of two parts, the conclusions drawn will be presented in two sections. In the first part, a 5 wt% Co-2 wt% Ce/ δ-Al_2O_3 catalyst was designed and tested in different temperatures, CH_4/CO_2 feed ratios and space velocities.

The major conclusions that can be drawn from the first part of this study can be given as follows:

- The SEM and XRD results revealed the well dispersion of Co and Ce with good homogeneity on freshly reduced 5 wt% Co-2 wt% Ce/δ-Al_2O_3 catalyst.
- EDS results confirmed the C formation on the spent catalyst. The results show that carbon deposition blocks the methane dehyrogenation sites and, as it covers the Ce sites, it also halts the surface oxygen transfer and carbon gasification mechanism.
- It was clearly observed that increasing temperature increased the activity although catalyst deactivation is relatively slower at low temperatures.
- For space velocity of 30000 mL/h g-catalyst no CDRM activity was observed. On the other hand, for the space velocities of 10000 mL/h g-catalyst and 20000 mL/h g-catalyst, almost the same performances were observed.
- The feed ratio of 1/2 yielded higher methane conversion and lower carbon dioxide conversion than those observed for the feed ratio of 1/1.

In the second part, 10 wt% Co-2 wt% Ce/ZrO_2 catalyst was prepared in order to investigate kinetic and mechanistic behavior of the reaction.

The major conclusions that can be drawn from the second part of this study can be given as follows:

- The SEM and XRD results revealed the uniform distribution of the freshly reduced 10 wt% Co-2wt% Ce/ZrO_2 catalyst.
- The activation energy of the reaction (E_A) is calculated as 61.3 kJ mol^{-1} K^{-1} for CH_4 and 50.53 kJ mol^{-1} K^{-1} for CO_2. The activation barrier for CH_4 is higher than that for CO_2 consumption, which is in agreement with reported values in the literature.
- The kinetics of CDRM over 10 wt% Co-2 wt% Ce/ZrO_2 catalyst can be expressed by a simple power-law rate equation, with reaction orders of 1.1926, -0.0968, for CH_4 and CO_2, respectively.
- The reaction orders indicated that the reaction rate was proportional to the partial pressure of methane while there is a small inhibition effect of carbon dioxide. This might be active site competition between CO_2 and CH_4 molecules, especially for the sites on which methane is activated.
- In the mixed feed tests, the correlation coefficients for the rate constants of CO and H_2 were found so small. Therefore, any observations about the effect of CO and H_2 partial pressures on CDRM rate could not be posibble.
- Increase of H_2 partial pressure led to a further CO_2 consumption which can be attributed to reverse water-gas shift reaction.
- An ER mechanism that has the reaction of adsorbed CO_2 with CH_4 from the gas phase leading directly to products, and an LH mechanism that has surface reaction of the adsorbed reactants to form products H_2 and CO ad the rate determining steps found plausible.
- The results clearly indicate that further FTIR-DRIFT analysis is necessary for finding the mechanism of CDRM reaction on Co-Ce/ZrO_2 system.

5.2. Recommendations

Considering the resulst of this experimental study, following ideas are suggested for future studies on CDRM:

- To prevent carbon deposition, an oxygen source can be added to the 5 wt% Co-2 wt% Ce/δ-Al_2O_3 system.
- The kinetic study can be performed over a wider range of partial pressures of reactants and products in order to observemore precise results. At least 2 more experiments should be added to mixed feed tests of CO partial pressure to make a more detailed analyse of its affect on CDRM mechanism.
- The structural characteristics of spent10 wt% Co-2 wt% Ce/ZrO_2 catalyst can be investigated.
- Catalysts can be prepared by coimpregnation method to estimate the effect of impregnation strategy on the reforming performance and kinetics.
- The effect of calcination and reduction temperature on the reforming activity can be investigated.

APPENDIX A: CONVERSION VERSUS RESIDENCE TIME GRAPHS

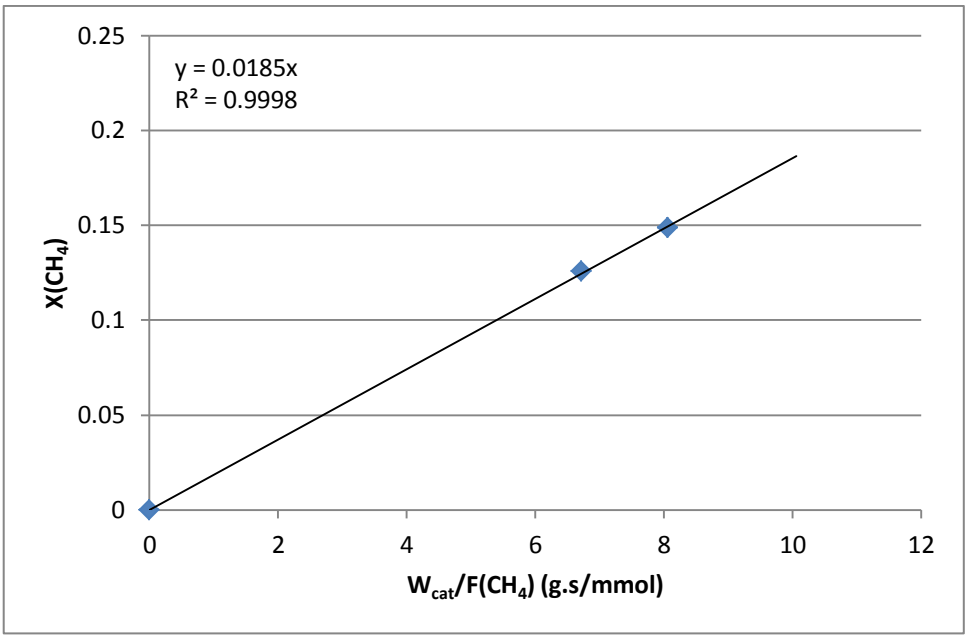

Figure A.1. Fractional CH_4 conversion vs. residence time graph of experiments 1-3.

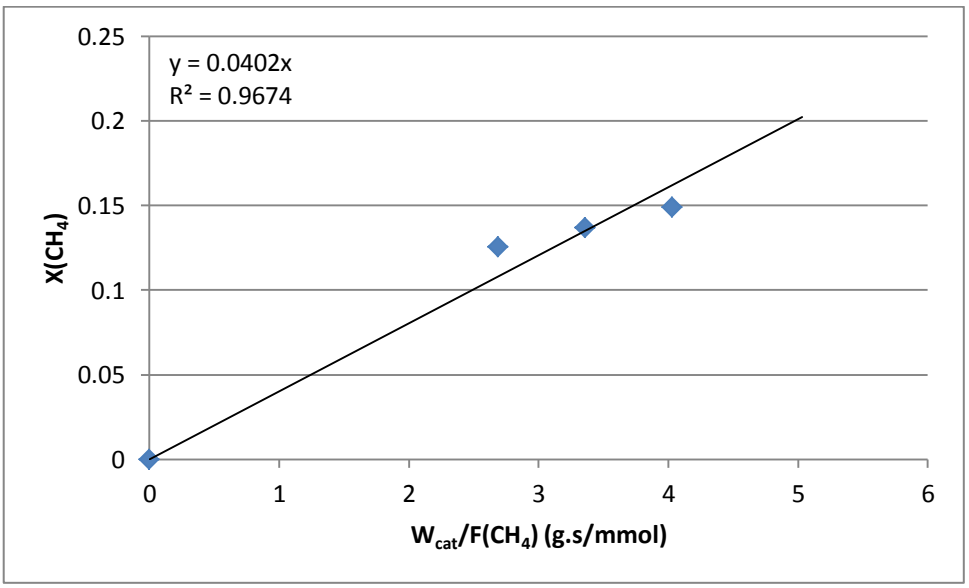

Figure A.2. Fractional CH_4 conversion vs. residence time graph of experiments 4-6.

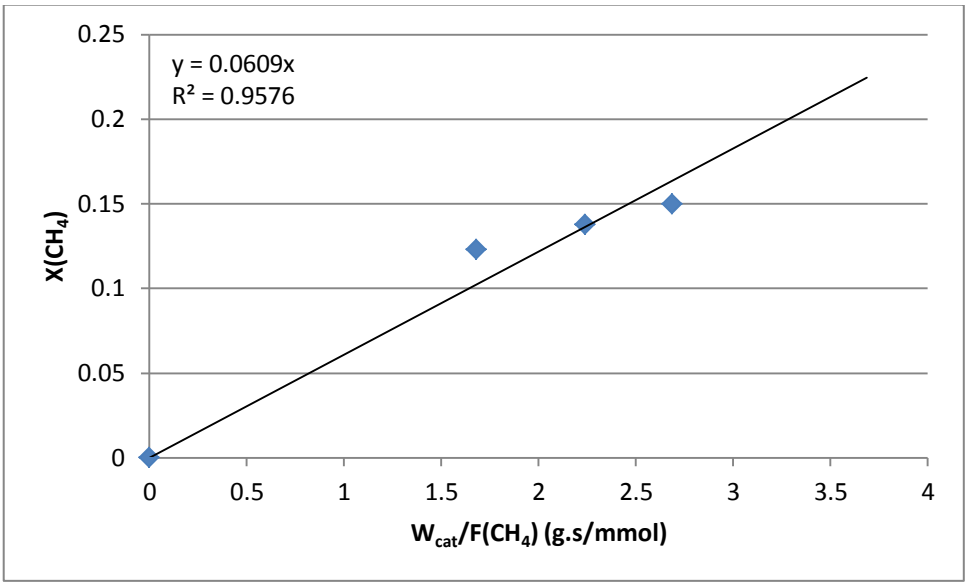

Figure A.3. Fractional CH_4 conversion vs. residence time graph of experiments 7-9.

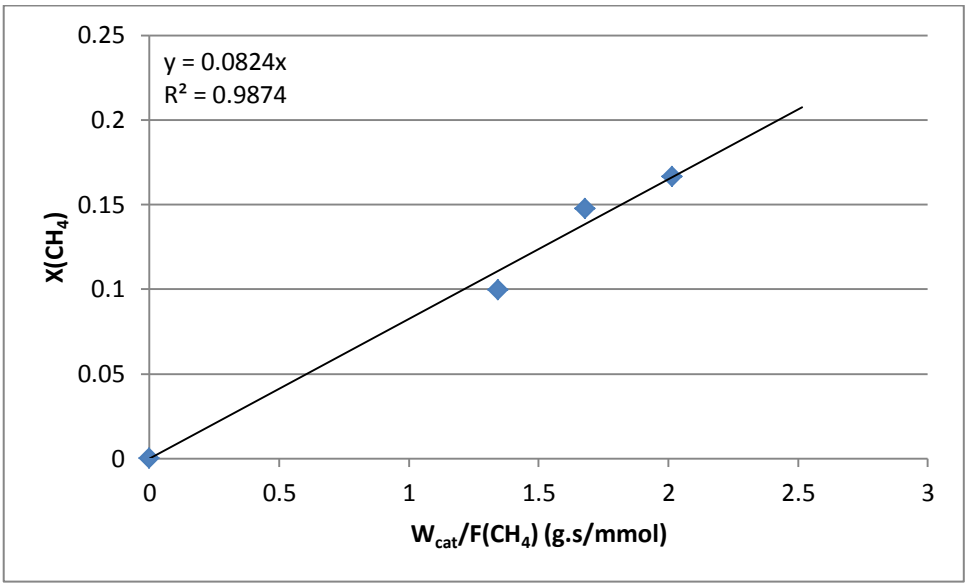

Figure A.4. Fractional CH_4 conversion vs. residence time graph of experiments 10-12.

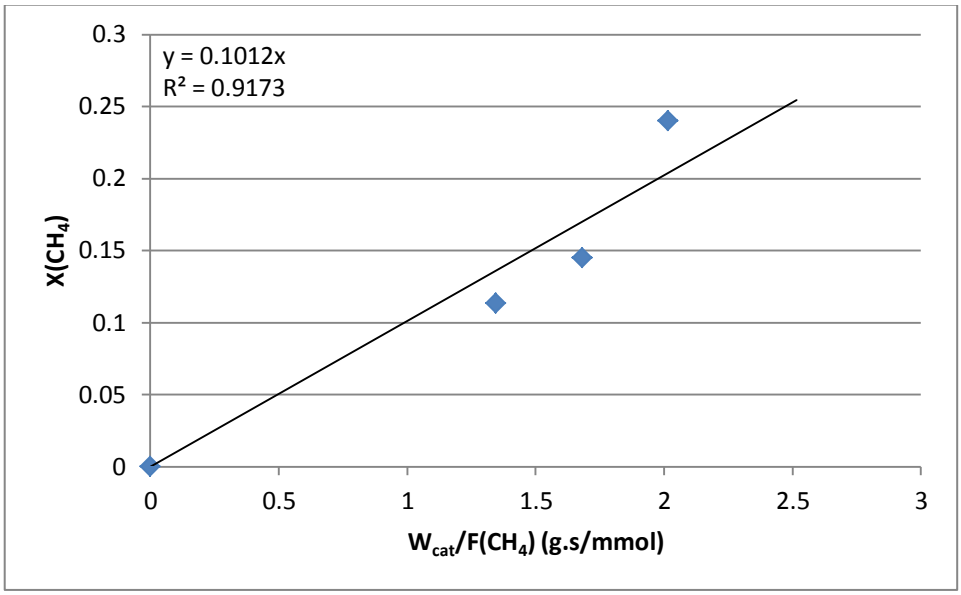

Figure A.5. Fractional CH_4 conversion vs. residence time graph of experiments 13-15.

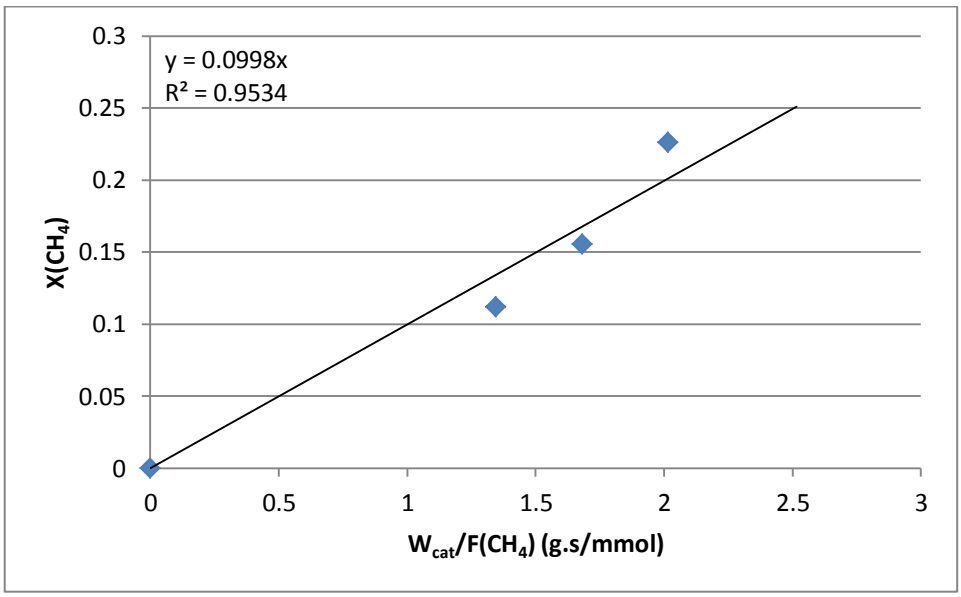

Figure A.6. Fractional CH_4 conversion vs. residence time graph of experiments 16-18.

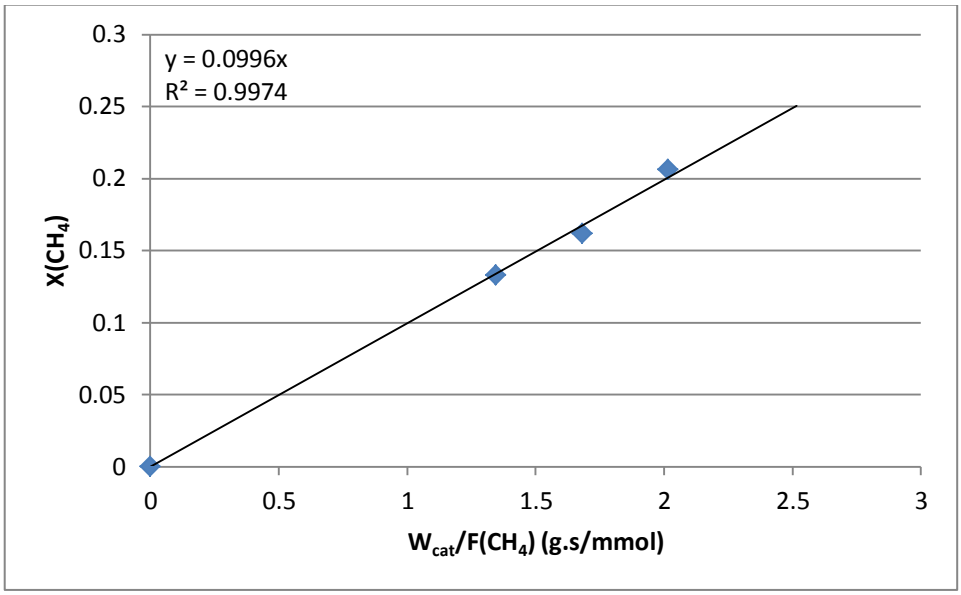

Figure A.7. Fractional CH_4 conversion vs. residence time graph of experiments 19-21.

APPENDIX B: EXPERIMENTAL AND CALCULATED REACTION RATES FOR POWER-LAW TYPE CDRM KINETICS

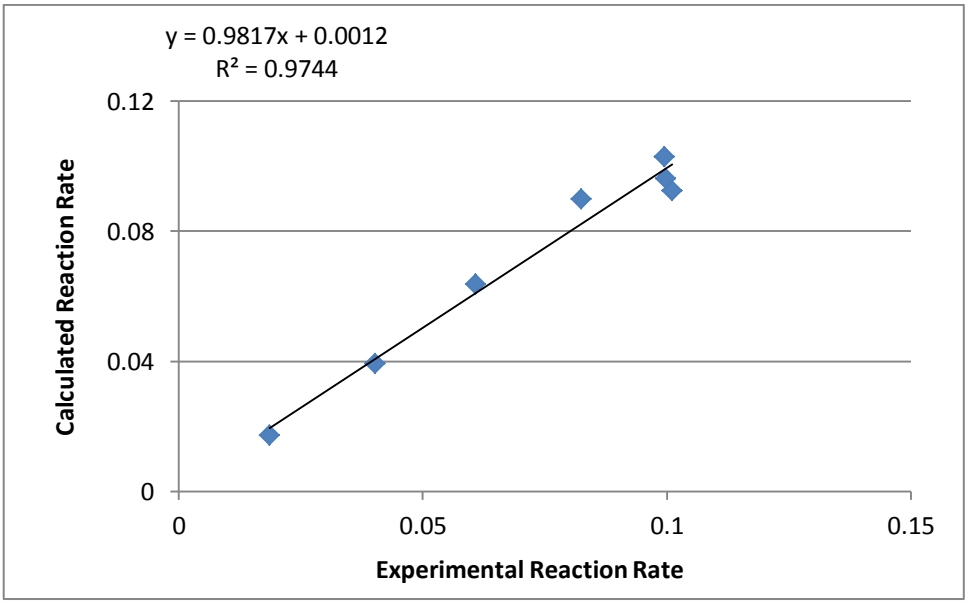

Figure B.1. Experimental and calculated reaction rates for power-law type CDRM kinetics.

APPENDIX C: CALCULATED MODEL PARAMETERS

Table C.1. Calculated Model Parameters.

Model No	Rate Parameters												σ^2 (mmol.g^{-1}.s^{-1})^2
	a	b	c	m	k	k_1	K_1	K_2	K_3	K_{CH_4}	K_{CO}	K_{CO_2}	
1	-	-	-	-	5.216	-	-	-	-	-	-	32.19	1.59×10^{-5}
2	-	-	-	-	-	0.8128	-0.0417	101.99	-	-	-	-	6.50×10^{-5}
3	2.345	5.511	0.0652	-	-	-	-	-	-	-	-	-	2.46×10^{-5}
4	-	-	-	-	64.586	-	-	-	-	0.0812	-	32.430	2.01×10^{-5}
5	-	-	-	-	-0.3719	-	-25.19	-25.19	-0.0086	-	-	-	1×10^{99}
6	-	-	-	-	-0.0584	-	-	-	-	-	-0.0140	-0.0076	4.97×10^{-5}
7	-	-	-	-0.122	48.941	-	-	-	-	0.0164	-	-	5.52×10^{-5}

APPENDIX D: EXPERIMENTAL AND CALCULATED REACTION RATES FOR MODELS

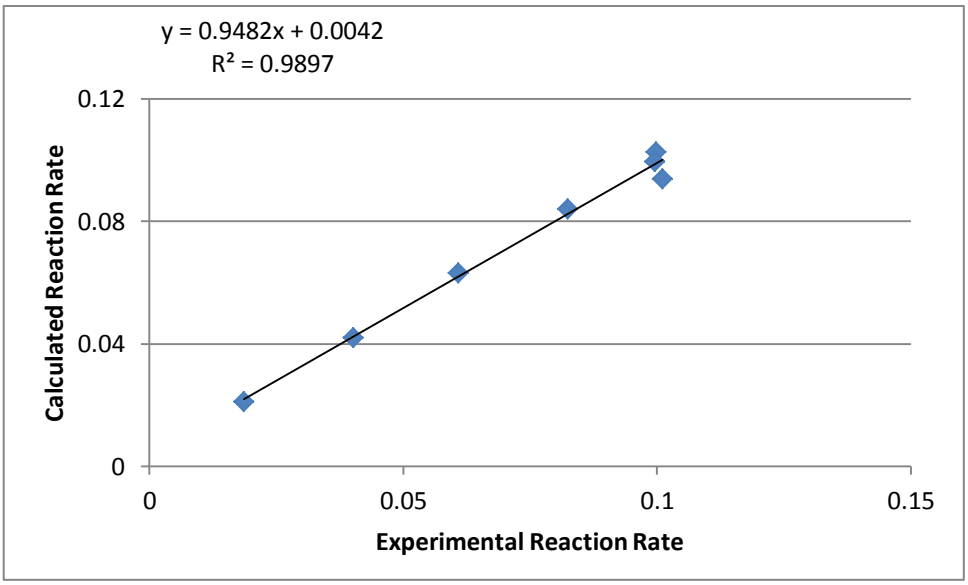

Figure D.1. Experimental and calculated reaction rates for Model 1.

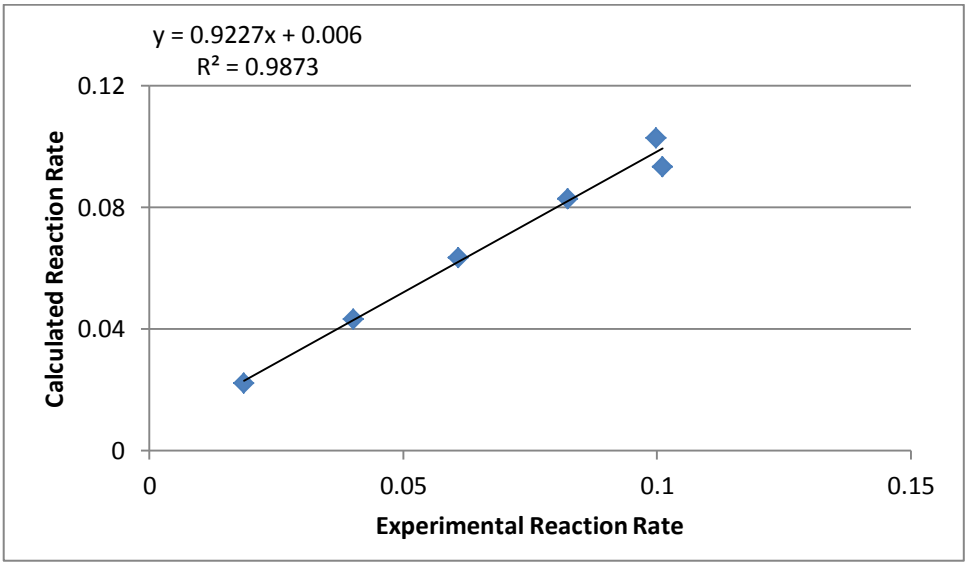

Figure D.2. Experimental and calculated reaction rates for Model 3.

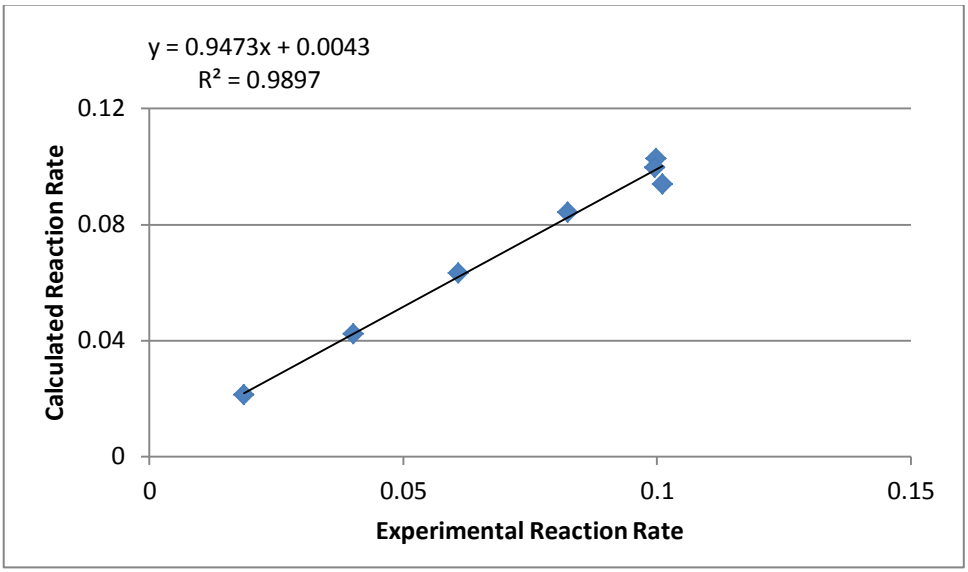

Figure D.3. Experimental and calculated reaction rates for Model 4.

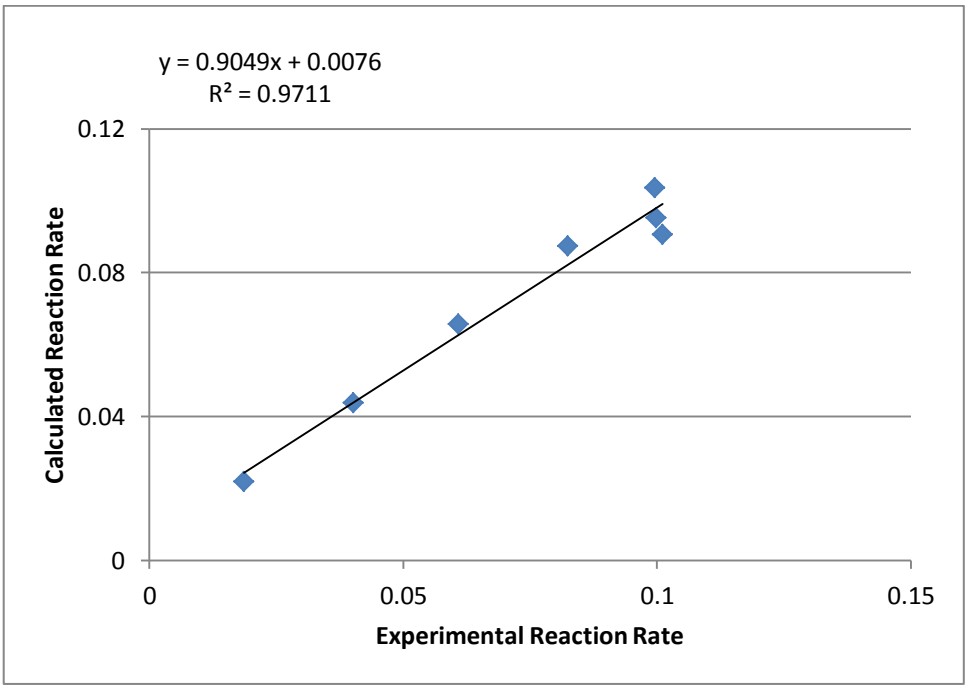

Figure D.4. Experimental and calculated reaction rates for Model 7.

REFERENCES

Akpan, E., Y. Sun, P. Kumar, H. Ibrahim, A. Aboudheir and R. Idem, 2007, "Kinetics, Experimental and Reactor Modeling Studies of the Carbon Dioxide Reforming of Methane (CDRM) over a New Ni/CeO_2–ZrO_2 Catalyst in a Packed Bed Tubular Reactor.", *Chemical Engineering Science*, Vol. 62, pp. 4012-4024.

Aksoylu, A. E., M. Madalena, A. Freitas, M. Fernando R. Pereira and J. L. Figueiredo, 2001, "The Effects of Different Activated Carbon Supports and Support Modifications on the Properties of Pt/AC Catalysts.", *Carbon*, Vol. 39, pp. 175–185.

Al-Fatesh, A. S. A., A. H. Fakeeha and A. E. Abasaeed, 2011, "Effects of Selected Promoters on Ni/γ-Al_2O_3 Catalyst Performance in Methane Dry Reforming", *Chinese Journal Of Catalysis*, Vol. 32, pp. 1604–1609.

Arkatova, L. A., 2010, "The Deposition of Coke During Carbon Dioxide Reforming of Methane over Intermetallides", *Catalysis Today*, Vol. 157, pp. 170–176.

Barroso-Quiroga, M. M. and A. E. Castro-Luna, 2010, "Catalytic Activity and Effect of Modifiers on Ni-based Catalysts for the Dry Reforming of Methane", *International Journal of Hydrogen Energy*, Vol. 35, pp. 6052- 6056.

Bartholomew, C. H., 2001, "Mechanisms of Catalyst Deactivation", *Applied Catalysis A: General*, Vol. 212, pp. 17–60.

Bradford, M. C. J. and M. A. Vannice, 1998, "CO_2 Reforming of CH_4 over Supported Pt Catalysts", *Journal of Catalysis*, Vol. 173, pp. 157-171.

Chen, J., C. Yao , Y. Zhao and P. Jia, 2010, "Synthesis Gas Production from Dry Reforming of Methane over $Ce_{0.75}Zr_{0.25}O_2$-Supported Ru Catalysts", *International Journal of Hydrogen Energy*, Vol. 35, pp. 1630–1642.

Cheng, J. and W. Huang, 2010, "Effect of Cobalt (Nickel) Content on the Catalytic Performance of Molybdenum Carbides in Dry-Methane Reforming", *Fuel Processing Technology*, Vol. 91, pp. 185–193.

Claridge, J. B., A. P. E. York, A.J. Brungs, C. Marquez-Alvarez, J. Sloan,S. C. Tsang and M. L. H. Green, 1998, "New Catalysts for the Conversion of Methane to Synthesis Gas: Molybdenum and Tungsten Carbide", *Journal of Catalysis*, Vol. 180, pp. 85-100.

Cui, Y., H. Zhang, H. Xu, W. Li, 2007, "Kinetic Study of the Catalytic Reforming of CH_4 with CO_2 to Syngas over Ni/α-Al_2O_3 Catalyst: The effect of temperature on the reforming mechanism", *Applied Catalysis A: General*, Vol. 318, pp. 79–88.

Damyanova, S., B. Pawelec, K. Arishtirova, M. V. Martinez Huerta and J. L. G. Fierro, 2009, "The Effect of CeO_2 on the Surface and Catalytic Properties of Pt/CeO_2-ZrO_2 Catalysts for Methane Dry Reforming", *Applied Catalysis B: Environmental*, Vol. 89, pp. 149–159.

Daza, C. E., S. Moreno and R. Molina, 2011, "Co-precipitated Ni–Mg–Al Catalysts Containing Ce for CO_2 Reforming of Methane", *International Journal of Hydrogen Energy*, Vol. 36, pp. 3886–3894.

Eltejaei, H., H. R. Bozorgzadeh, J. Towfighi, M. R. Omidkhah , M. Rezaei, R. Zanganeh, A. Zamaniyan and A. Z. Ghalam, 2012, "Methane Dry Reforming on Ni/$Ce_{0.75}Zr_{0.25}O_2$–$MgAl_2O_4$ and Ni/$Ce_{0.75}Zr_{0.25}O_2$–γ-alumina: Effects of Support Composition and Water Addition", *International Journal of Hydrogen Energy,* Vol. 37, pp. 4107–4118.

Er-rbib, H., C. Bouallou and F. Werkoff , 2012, "Production of Synthetic Gasoline and Diesel Fuel from Dry Reforming of Methane", *Energy Procedia,* Vol. 29, pp. 156 – 165.

Fan, M.-S., A. Z. Abdullah and S. Bhatia, 2011, "Hydrogen Production from Carbon Dioxide Reforming of Methane over Ni-Co/MgO-ZrO_2 Catalyst: Process Optimization*", International Journal of Hydrogen Energy*, Vol. 36, pp. 4875-4886.

Fidalgo, B., L. Zubizarreta, J. M. Bermúdez, A. Arenillas and J.A. Menéndez, 2010, "Synthesis of Carbon-Supported Nickel Catalysts for the Dry Reforming of CH_4", *Fuel Processing Technology*, Vol. 91, pp. 765–769.

Gangadharan, P., K. C. Kanchi and H. H. Lou, 2012, "Evaluation of the Economic and Environmental Impact of Combining Dry Reforming with Steam Reforming of Methane", *Chemical Engineering Research and Design*, Vol. 90, pp. 1956–1968.

Guerrero-Ruiz, A., A. Sepúlveda-Escribano and I. Rodríguez-Ramos, 1994, "Cooperative Action of Cobalt and MgO for the Catalysed Reforming of CH_4 with CO_2", *Catalysis Today*, Vol. 21, pp. 545-550.

Juan-Juan, J., M. C. R. Martinez and M. J. Illan-Gomez, 2009, "Nickel Catalyst Activation in the Carbon Dioxide Reforming of Methane: Effect of Pretreatments", *Applied Catalysis A: General*, Vol. 355, pp. 27–32.

Kambolis, A., H. Matralis, A. Trovarelli and Ch. Papadopoulou, 2010, "Ni/CeO_2-ZrO_2 Catalysts for the Dry Reforming of Methane", *Applied Catalysis A: General*, Vol. 377, pp.16–26.

Kang, K.-M., H.-W. Kim, I.-W. Shim and H.-Y. Kwak, 2011, "Catalytic Test of Supported Ni Catalysts with Core/Shell Structure for Dry Reforming of Methane" *Fuel Processing Technology*, Vol. 92, pp. 1236–1243.

Laosiripojana, N. and S. Assabumrungrat, 2005, "Catalytic Dry Reforming of Methane over High Surface Area Ceria", *Applied Catalysis B: Environmental*, Vol. 60, pp. 107–116.

Laosiripojana, N., W. Sutthisripok and S. Assabumrungrat, 2005, "Synthesis Gas Production from Dry Reforming of Methane over CeO_2 Doped Ni/Al_2O_3: Influence of the Doping Ceria on the Resistance toward Carbon Formation", *Chemical Engineering Journal*, Vol. 112, pp.13–22.

Lee, J.-H., Y.-W. You, H.-C. Ahn, J.-S. Hong, S.-B. Kim, T.-S. Chang and J.-K. Suh, 2013, "The Deactivation Study of Co–Ru–Zr Catalyst Depending on Supports in the Dry Reforming of Carbon Dioxide" *Journal of Industrial and Engineering Chemistry*.

Li, X., Q. Hua, Y. Yanga, Y. Wanga and F. Heb, 2012, "Studies on Stability and Coking Resistance of $Ni/BaTiO_3$–Al_2O_3 Catalysts for Lower Temperature Dry Reforming of Methane (LTDRM)", *Applied Catalysis A: General*, Vol. 413– 414, pp. 163– 169.

Liu, D., X. Y. Quek, W. N. E. Cheo, R. Lau, A. Borgna and Y. Yang, 2009, "MCM-41 Supported Nickel-based Bimetallic Catalysts with Superior Stability During Carbon Dioxide Reforming of Methane: Effect of Strong Metal–Support Interaction", *Journal of Catalysis*, Vol. 266, pp. 380–390.

Luisetto, I., S. Tuti and E. D. Bartolomeo, 2012, "Co and Ni Supported on CeO_2 as Selective Bimetallic Catalyst for Dry Reforming of Methane", *International Journal of Hydrogen Energy*, Vol. 37, pp. 15992–15999.

Miguel, S.R. , I.M.J. Vilella, S.P. Maina, D. S. José-Alonso, M.C. Román-Martínez and M.J. Illán-Gómez, 2012, "Influence of Pt Addition to Ni Catalysts on the Catalytic Performance for Long Term Dry Reforming of Methane", *Applied Catalysis A: General* Vol. 435-436, pp.10-18.

Nagai, M., K. Nakahira, Y. Ozawa, Y. Namiki and Y. Suzuki, (2007), "CO_2 Reforming of Methane on Rh/Al_2O_3 Catalyst", *Chemical Engineering Science*, Vol. 62, pp. 4998-5000.

Nandini, A., K.K. Pant and S.C. Dhingra, 2006, "Kinetic Study of the Catalytic Carbon Dioxide Reforming of Methane to Synthesis Gas over Ni-K/CeO_2-Al_2O_3 Catalyst", *Applied Catalysis A: General,* Vol.308, pp. 119-127.

Nematollahi, B., M. Rezaei and M. Khajenoori, 2011, "Combined Dry Reforming and Partial Oxidation of Methane to Synthesis Gas on Noble Metal Catalysts*",* *International Journal of Hydrogen Energy*, Vol. 36, pp. 2969-2978.

Newnham, J., K. Mantri, M. H. Amin, J. Tardio and S. K. Bhargava, 2012, "Highly Stable and Active Ni-mesoporous Alumina Catalysts for Dry Reforming of Methane", *International Journal of Hydrogen Energy*, Vol. 37, pp. 1454–1464.

Ocsachoque, M., F. Pompeo and G. Gonzalez, 2011, "Rh–Ni/CeO_2–Al_2O_3 Catalysts for Methane Dry Reforming", *Catalysis Today*, Vol. 172, pp. 226– 231.

Omata, K., N. Nukui, T. Hottai and M. Yamada, 2004, "Cobalt–Magnesia Catalyst by Oxalate Co-precipitation Method for Dry Reforming of Methane Under Pressure", *Catalysis Communications*, Vol. 5, pp. 771–775.

Omata, K., N. Nukui, T. Hottai, Y. Showa and M. Yamada, 2004, "Strontium Carbonate Supported Cobalt Catalyst for Dry Reforming of Methane under Pressure", *Catalysis Communications*, Vol. 5, pp. 755–758.

Ozkara-Aydinoglu, S. and A. E. Aksoylu, 2010, "CO_2 Reforming of Methane over Pt–Ni/Al_2O_3 Catalysts: Effects of Catalyst Composition, Water and Oxygen Addition to the Feed", *International Journal of Hydrogen Energy*, Vol. 36, pp. 2950–2959.

Ozkara-Aydinoglu, S., A. E. Aksoylu, 2010, " Carbon Dioxide Reforming of Methane over Co-X/ZrO_2 Catalysts (X=La, Ce, Mn, Mg, K)", *Catalysis Communications*, Vol. 11, pp. 1165–1170.

Ozkara-Aydınoglu, S., E. Ozensoy and A. E. Aksoylu, 2009, "The Effect of Impregnation Strategy on Methane Dry Reforming Activity of Ce Promoted Pt/ZrO_2", *International Journal of Hydrogen Energy*, Vol. 34, pp. 9711–9722.

Ozkara-Aydinoglu, S., *Utilization of Carbon Dioxide and Methane via Catalytic Reforming Reactions*, Ph.D. Thesis, Bogazici University, 2008.

Reddy, G. K., S. Loridanta, A. Takahashi, P. Delichère and B. M. Reddy, 2010, "Applied Reforming of Methane with Carbon Dioxide over $Pt/ZrO_2/SiO_2$ Catalysts- Effect of Zirconia to Silica Ratio", *Catalysis A: General*, Vol. 389, pp. 92-100.

Rezaei, M., S. M. Alavi, S. Sahebdelfar and Z. Yan, 2007, "Mesoporous Nanocrystalline Zirconia Powders: A Promising Support for Nickel Catalyst in CH_4 Reforming with CO_2", *Materials Letters*, Vol. 61, pp. 2628-2631.

Ruckenstein, E. and H. Y. Wang, 2002, "Carbon Deposition and Catalytic Deactivation during CO_2 Reforming of CH_4 over $Co/\gamma\text{-}Al_2O_3$ Catalysts", *Journal of Catalysis*, Vol. 205, pp. 289–293.

Ruckenstein, E. and H.Y. Wang, 2000, "Carbon Dioxide Reforming of Methane to Synthesis Gas over Supported Cobalt Catalysts", *Applied Catalysis A: General*, Vol. 204, pp. 257–263.

San-Jose´-Alonso, D., J. Juan-Juan, M.J. Illa´n-Go´ mez and M.C. Roma´ n-Martı´nez, 2009, "Ni, Co and Bimetallic Ni–Co Catalysts for the Dry Reforming of Methane", *Applied Catalysis A: General*, Vol. 371, pp. 54–59.

Souza, M. M. V. M., D. A. G. Aranda and M. Schmal, 2001, "Reforming of Methane with Carbon Dioxide over $Pt/ZrO_2/Al_2O_3$ Catalysts", *Journal of Catalysis*, Vol. 204, pp.498-511.

Stagg-Williams, S. M., F. B. Noronha, G. Fendley and D. E. Resasco, 2000, "CO_2 Reforming of CH_4 over Pt/ZrO_2 Catalysts Promoted with La and Ce Oxides", *Journal of Catalysis*, Vol. 194, pp. 240-249.

Steinhauer, B., M. R.Kasireddy, J. Radnik and A. Martin, 2009, " Development of Ni-Pd Bimetallic Catalysts for the Utilization of Carbon Dioxide and Methane by Dry Reforming" *Applied Catalysis A: General*, Vol.366, pp. 333–341.

Wang, N., W. Chu, L. Huang and T. Zhang, 2010, "Effects of Ce/Zr Ratio on the Structure and Performances of Co-Ce_{1-x} Zr_xO_2 Catalysts for Carbon Dioxide Reforming of Methane", *Journal of Natural Gas Chemistry*, Vol. 19, pp. 117–122.

Wang, N., W. Chu, T. Zhang and X.-S. Zhao , 2011, "Manganese Promoting Effects on the Co–Ce–Zr–O_x Nano Catalysts for Methane Dry Reforming with Carbon Dioxide to Hydrogen and Carbon Monoxide", *Chemical Engineering Journal*, Vol. 170, pp. 457–463.

Wang, S.-G.,Y.-W. Li, J.-X. Lu, M.-Y. He and H. Jiao, 2004, "A Detailed Mechanism of Thermal CO_2 Reforming of CH_4", *Journal of Molecular Structure*, Vol.673, pp.181–189.

Xu, L., H. Song and L. Chou, 2011, "Carbon Dioxide Reforming of Methane over Ordered Mesoporous NiO–MgO–Al_2O_3 composite oxides" *Applied Catalysis B: Environmental*, Vol. 108– 109, pp. 177– 190.

Yao, L., J. Zhu, X. Peng, D. Tong and C. Hu, 2013, "Comparative Study on the Promotion Effect of Mn and Zr on the Stability of Ni/SiO_2 Catalyst for CO_2 Reforming of Methane", *International Journal of Hydrogen Energy*, Vol. 38, pp. 7268–7279.